CENTRO DE INVESTIGACIÓN EN MATERIALES AVANZADOS S. C.

ACADEMIC UNIT OF POSTGRADE STUDIES

"SYNTHESIS AND CHARACTERIZATION OF PANI / GRAPHENE COMPOSITES"

A THESIS SUBMITTED IN FULLFILLMENT OF THE REQUIREMENTS FOR THE AWARD OF THE DEGREE

DOCTOR OF PHILOSOPHY IN MATERIALS SCIENCE

BY

ELÇiN COŞKUN

Thesis Director: Erasto Armando Contreras Zaragoza

February 20, 2012. C

"There are only two mistakes one can make along the road to truth; not going all the way, and not starting."

Buddha

ABSTRACT

The PAni/Graphene composites by two different methods are studied. In the first method, graphene oxide is used as the dopant of polyaniline taking the advantage of GO makes itself as a dopant to polyaniline (PAni) due to its carboxylic acids on its surface. According to that idea graphene oxide (GO) is reduced by leucoemeraldine state of PAni, instead of using another reducing agent both to remove oxygene functionality on the graphite oxide and oxide the PAni in leucoemeraldine state to the conducting emeraldine state. PAni/reduced graphene (PAni/RGO) with different mass ratio is prepared. For comparison, PAni/GO composites also is prepared by *in situ* polymerization of polyaniline. The composites have been characterized by Fourier Transform Infrared Spectrum (FTIR spectroscopy), UV-visible (UV-VIS) spectroscopy and cyclic voltammetry (CV).

FTIR spectroscopy of the PAni/RGO materials showed the typical peaks of the PAni which can be concluded the presence of PAni in the composites. The characteristic peaks of the GO were not observed. It was the direct evidence of the removal of the oxygene functional groups. UV-VIS spectroscopy indicated the same results as FTIR. According to the results, the leucoemeraldine state of PAni oxided to emeraldine state while GO reduced.

CV studies showed that the materials are electrochemically active. The electrochemical performances were affected by the mass ratio PAni : RGO. The electrochemical performances of the PAni / RGO 100 exhibits closer electrochemical performance to PAni. According to the four-probe technique the electrical conductivity of the materials

were 0. 845, 0. 44, 0. 279, 0. 06, 0. 05, 0. 02 S cm^{-1} for PAni, PAni / GO, PAni / RGO 100, PAni / RGO 200, PAni / RGO 300, and PAni / RGO 500 respectively.

As a second method, the sulfonation of graphene by two different strategies is studied. Hybrids of PAni and sulfonated graphene (SGrf) are prepared by the polymerization of aniline in the presence of the SGrf . The materials have been characterized by RAMAN spectroscopy, FTIR spectroscopy, thermogravimetric analyse (TGA) , CV and Transmission Electron Microscopy (TEM).

Raman spectroscopy results used to calculate D / G intensities of sulfonated graphenes. The results for reduced and sulfonated graphene sheets by sulfonic acid (GSA) and reduced and sulfonated graphene sheets by 6-amino-4-hydroxy-2-naphthalenesulfonic acid (GNSA) and GO samples were 0.96, 0.92 and 0.87 respectively which indicates the formation of smaller graphitic domains than those in GO and graphene-oxide reduction.

FTIR spectroscopy of the PAni/ SGrf s showed that clear bands at 1095 and 1037 cm^{-1}, which are assigned to the symmetric and anti-symmetric stretching of sulfonic groups respectively which points to successful sulfonation of the graphenes. UV-VIS spectroscopy was used to calculate water solubility of the sulfonated graphenes. According to the results, the solubilities of the GSA and GNSA samples were 0. 104 and 0. 138 mg mL^{-1} respectively.

TGA indicated that less volatile functionalities are present on GSA and GNSA surfaces comparing to GO as a result of the successful reduction. This pointed to sulfonation method was the efficient way to obtain more thermostable compositions.

TEM results showed typical-wrinkled morphology of the reduced-sulfonated graphene sheets. Morphologies of the PAni/ SGrf showed the particles of PAni intercalated/covered on the surfaces of the graphene sheets. According to the EDS results the ratio of sulfur element was % 5. 78 in the GNSA sample. It is a good indicator of the sulfonation efficiency.

The CV results showed that the materials are electrochemically active at physiological pH likely due to the doping of PAni with SGrf. . In fact, a good electrochemical response is obtained at pH 6 for the PAni/ SGrf s. In addition high conductivity values are obtained by four probe technique. The electrical conductivities were 1. 42, 13. 60, 14. 09, 25. 60, 26. 33 S cm^{-1} for PAni, GSA, GNSA, PAni/ GSA, PAni/ GNSA samples respectively.

General results indicated that the both method was efficient to obtain electrochemically active and electrically conductive materials. This let us the conclude that methods of the dopping the polyaniline with graphene oxide and funcionalization of the polyaniline with the modified graphenes worked very well. The sulfonation method was prominent as higher conductivities obtained compare to pure PAni due to surface modificated graphenes provides better interconnection with PAni as it was stated in the hypotheses.

TABLE OF ABBREVIATIONS

PAni	**Polyaniline**
GO	Graphene oxide
RGO	Reduced graphene oxide
PAni / RGO	Polyaniline-reduced graphene oxide composite
PAni / GO	Polyaniline-graphene oxide composite
SGrf (s)	Sulfonated and reduce graphene (s)
GSA	Reduced graphene oxide sheets sulfonated by sulfonic acid
GNSA	Reduced graphene oxide sheets sulfonated by 6-amino-4-hydroxy-2-naphthalenesulfonic acid
PAni/ GSA	Polyaniline dopped reduced graphene oxide sheets sulfonated by sulfonic acid composite
PAni/GNSA	Polyaniline dopped reduced graphene oxide sheets sulfonated by 6-amino-4-hydroxy-2-naphthalenesulfonic acid

OUTLINE

ABSTRACT

CHAPTER I 1

I. INTRODUCTION 1

II. BACKGROUND 4

a. Conductive Polymers 4

b. Polyaniline 5

c. Graphene 10

d. PAni / Graphene composites 14

III. JUSTIFICATION 18

IV. HYPOTHESES 18

V. OBJECTIVE 19

Particular Objectives 19

CHAPTER II 21

VI. THEORITICAL ASPECTS 21

POLYANILINE 21

Polyaniline Synthesis 22

The doping mechanism of polyaniline and the conductivity 23

GRAPHENE 23

Structural Features 24

Conductivity in Graphene 25

From graphite to graphite oxide, from graphite oxide to graphene 26

Functionalization of Graphene 28

Method 1: 32

General procedure for the synthesis of emeraldine salt of PANI 32

Synthesis of chemically reduced PANI (leucoemeraldine salt of PANI): 32

Synthesis of PAni / reduce Go (RGO) 33

Preparation of PAni / GO composites 33

Method 2. 34

Preparation of sulfonated graphene (SGrf). 34

Synthesis of PAni/ sulfonated graphene (PAni/ SGrf) 34

VIII. CHARACTERIZATION 35

INFRARED SPECTROSCOPY 35

UV-VIS SPECTROSCOPY 35

RAMAN SPECTROSCOPY 35

TEM 36

TGA 36

CYCLIC VOLTAMMETRY 36

CONDUCTIVITY MEASUREMENT BY FOUR-PROBE TECHNIQUE 37

CHAPTER III 39

IX. RESULTS AND DISCUSSION 39

PART 1 39

POLYANILINE / RGO COMPOSITES 39

POLYANILINE/GO COMPOSITES 40

1. UV-VIS and FT-IR spectra 41

2. Cyclic voltammetry 44

PART 2 48

Modification of reduced graphene 48

In situ polymerization of polyaniline 49

1. UV-VIS and FT-IR spectra 50

2. Tga 56

3. Raman Spectroscopy 57

4. Cyclic Voltammetry Studies 59

4. 1. Sensor Application 69

5. Morphology Studies 71

X. CONCLUSIONS 76

REFERENCES 77

FIGURE CAPTION

Figure 1. Formation of aniline radical 6

Figure 2. Representation of polyaniline: from insulator to conductor by oxidation; from conductor to insulator by reduction. 7

Figure 3. Conversion mechanism of polyaniline 22

Figure 4. The conventional synthesis of polyaniline 23

Figure 5: All graphitic forms 25

Figure 6: TEM images and hexagonal atomic arrangement of graphene nanosheets 25

Figure 7. Electron hopping mechanism in valence electrons of graphene 26

Figure 8. Graphite oxidation 27

Figure 9. Oxidized graphite 27

Figure 10. Reducing graphene by hydrazine 29

Figure 11. Simultaneous oxidation of polyaniline 30

Figure 12. Incorporation of the sulfonated graphene onto PAni 30

Figure 13: Four probe method 38

Figure 14: Proposed equation of oxidation of leucoemeraldine state of PAni by reduction of GO 40

Figure 15. GO dopped polyaniline (PANI/GO) 40

Figure 16. UV-VIS spectra of the PAni, PAni / RGO, and GO samples 42

Figure 17. FT-IR spectra of pure PANI, GO, PANI/RGO and PANI/GO 42

Figure 18. Voltammograms at 100 mV s^{-1} 45

Figure 19. Cyclic voltammograms of the PAni / RGO 100 composite at different scan rates 46

Figure 20. Sulphanilic acid and reduced graphene sheets 48

Figure 21. 6-amino-4-hydroxy-2-naphthalenesulfonic acid and graphene sheets. 49

Figure 22 : RGO-SA dopped polyaniline (PANI/GSA) 49

Figure 23. RGO-NSA dopped polyaniline (PANI/GNSA) 50

Figure 24. UV-VIS spectra of the PAni, PAni / GSA, and PAni / GNSA 50

Figure 25. UV-VIS spectra of the doped PAni, PAni / GSA, and PAni / GNSA 52

Figure 26. UV-VIS spectrum of the GSA and GNSA in water 53

Figure 27. FT-IR spectra of the PAni-sulfonated graphene composites 55

Figure 28. FT-IR spectra of the GSA and GNSA materials 56

Figure 29. TGA curves of GO, GSA and GNSA 56

Figure 30. Raman spectra of the GO, GSA, and GNSA 58

Figure 30. Cyclic voltammograms of a) PAni / GSA, and b) PAni / GNSA composites at different scan rates. 60

Figure 31. Conversion from emeraldine salt to pernigraniline 61

Figure 32. CV voltammograms of the composites until 0. 6 V 62

Figure 33. Cyclic voltammograms of a) pure PAni, b) PAni / GSA, and c) PAni / GNSA in different pHs at 20 mV. s^{-1} 63

Figure 34. 2nd oxidation potentials *versus* pH values of the composites 66

Figure 35. The relationship between the maximum oxidation peak currents and scan rate, the relationship between the maximum oxidation peak current, and the square roots of the scan rate in PAni / SGrfs 67

Figure 36. Cyclic voltammograms of PAni/GSA composite electrodes in phosphate buffers (pH = 6) + 1mM ferrocenium solution at different scan rates. 69

Figure 37. Cyclic voltammograms of PAni / GSA and PAni / GNSA materials in phosphate buffers (pH = 6) and 1 mM ferrocenium solution in phosphate buffers pH 6 70

Figure 38. High resolution micrographs of GSA at different magnitude. 71

Figure 39. a) Graphene sheets reduced by $KBrH_4$ b) GNSA..... 72

Figure 40. TEM images of the GNSA composites. (a) Zero-energy loss bright field image, (b) carbon element mapping, (c) sulfur element mapping..... 72

Figure 41. TEM image of the GNSA composite 73

Figure 42. Electron diffraction pattern of the selected areas of the GNSA composite ... 74

Figure 43. TEM images of the PAni/GNSA composites 75

Figure 44. TEM images of PAni/GSA composite..... 76

TABLE LIST

Table 1. Specific capacities of the materials 47

Table 2. Potential values at 1^{st} and 2^{nd} oxidation conversions 65

Table 3. Dependence of the peak potential on pH for second redox processes. 67

Table 4. Electrical conductivity of the products 68

Table 5. Elemental analysis of the selected areas in Figure 41 73

CHAPTER I

I. INTRODUCTION

Materials science can be divided into different groups in relation to their compositions, for example: ceramics, glasses, metals, or plastics. Plastics are typically organic polymers of high molecular mass; they are usually synthetic, most commonly derived from petrochemicals, but many are partially natural. Composite materials often called composites are engineered or naturally occurring materials, made from two or more constituent materials with significantly different physical or chemical properties. Semiconductors are materials with electrical conductivity intermediate in magnitude between that of a conductor and an insulator. Common semiconducting materials are crystalline solids, but amorphous and liquid semiconductors are also known. Silicon is used to create most semiconductors commercially.

In the last years, the area of the science and technology has been directed towards the study of synthetic metals. Synthetic metals are man-made materials that have many of the properties of metals, they conduct electricity, they can be magnetic, and they can be stimulated to produce light and so on (Macdiarmid, 2001). The common synthetic metals are the derivates of carbon and conducting polymers. They have applications in an extremely diverse range of areas such as artificial muscles, electronic noses, plastic solar cells, light emitting diodes, corrosion inhibition, biological and chemical sensors, electronic textiles and nerve cell communications (Potts, 2011).

Carbon compounds are creating the strongest materials ever known by humans, by adopting a variety of forms, such as graphite, diamond, fullerenes, carbon nanotubes and graphene. The reason that it assumes many different structural forms is that carbon atom forms several distinct types of valance bonds, which refers to hybridization of atomic orbitals (Falcao and Wudl, 2007). Because of their different atomic conFigureuration, graphite, graphene, and diamonds are named as allotropes of carbon. Graphite is a common structure of carbon atoms that consists of multiple layers of carbon atoms arranged in a honeycomb lattice. In diamond, the carbon atoms are arranged in a variation of the face-centered cubic crystal structure, called a diamond lattice. Graphene is a single atomic layer of this honeycomb lattice, which is composed of carbon atoms that form hexagonal rings. Graphene is thin, a very good electric conductor, a good thermal conductor, transparent, and is highly impermeable (Fuhrer *et al.* , 2010). Graphene´s honeycomb lattice sheets of carbon can be wrapped up to create fullerenes that are shaped like a soccer ball, rolled to create nanotubes, or layered to create graphite. The outstanding properties of graphene, such as higher electron mobility, large specific surface area, mechanical strength have catapulted it to be one of the most studied and promising materials for the coming years.

Almost invariably, organic polymers mainly comprise plastics. The vast majority of these polymers are based on chains of carbon atoms alone or with oxygen, sulfur, or nitrogen as well. The properties of plastics are defined chiefly by the organic chemistry of the

polymer such as hardness, density and resistance to heat, organic solvents, oxidation, and ionizing radiation. Some plastics can be made electrically conductive, with the conductivity of up to 80 kS/cm like in polyacetylene (Kumar *et al.* , 2011). They are called as conductive polymers or, more precisely, intrinsically conducting polymers (ICPs). They are polymers that conduct electricity linear-backbone "polymer blacks" (polyacetylene, polypyrrole, and polyaniline) and their copolymers are the main class of conductive polymers. Conductive polymers are well known for their low ionization potential, and high electron affinity due their π-electron backbone (Gerard *et al.* , 2002). The term of “synthetic metals” refers to conductive polymers due their electrical conductivity. Excitement about these polymeric materials is evidenced by the fact that the field of conducting polymers has attracted scientists from such diverse areas of interest as synthetic chemistry, electrochemistry, solid-state physics, materials science, polymer science, electronics and electrical engineering with their applications in solar cells, light weight batteries, electrochromic devices molecular electronic devices and sensors (Manju *et al.* , 2002). Polyaniline is one of the most compromised intrinsic electrical conductive materials due to its environmental stability, easy to synthesis, good electrical conductivity and uncommon conducting / insulating fast transition by doping / dedoping process and low cost (Bhadra *et al.* , 2009; Yang *et al.* , 2010). These capabilities make them ideally suited for use in electrical devices.

In the modern world, plastics and carbenous materials are always tightly integrated. Up to now, most of the studies devoted to the realization of conducting materials using polyaniline and carbenous materials. These materials have been mostly oriented

towards the synthesis of graphene and polyaniline using insitu polymerization technique, aniodic polymerization technique, electropolymerization technique, etc (Wang *et al.* , 2009; Gospadinova and Terlemezyan, 1998). Unfortunately, the low efficiency of the functionalization between the polyaniline and graphene, have limited some of their potential applications like sensing, capacitor, actuators, etc (Bai *et al.* , 2009)

This investigation intends to conduct preliminary work towards the functionalization of graphene with the polyaniline. There is much anticipation that growth in the availability of polyaniline / graphene composite materials, and improvements in electrical conductivity, electrochemical activity, thermal properties, will lead to advancements in the field of developing commercially viable sensor, capacitor, etc.

II. BACKGROUND

a. Conductive Polymers

Until about 40 years ago, all carbon based polymers were rigidly regarded as insulators. They were utilized as inactive packaging and insulating material. At the start of the 60's, the research priorities at the Plastics Research Laboratory of BASF in Ludwigshafen, Germany, centered on postulating new structural properties of polymers made by oxidative coupling. Copper chloride and aluminium chloride were used to make oligo-benzene from benzene (Shirakawa, 2001). This reaction was extended to include other aromatic compounds and heterocycles. These reaction products were characterized in terms of thermoelectric power, and photo- and dark conductivities. To their surprise polyphenylene and polythiophene showed electrical conductivities of up to 0. 1 S cm^{-1}

(Shirakawa, 2001). Not only was this the highest value yet obtained, but it was the first capable of conducting electricity. Research interest in electroactive polymers started in 1977, when Heeger, MacDiarmid, Shirakawa and their co-workers demonstrated that the conductivity of polyacetylene—the simplest polyene—can be increased by several orders of magnitude by treatment with appropriate oxidizing or reducing agents, the so-called 'dopants' (Shirakawa *et al.* , 1977). These scientists were awarded the Nobel Prize in Chemistry in 2000 for the discovery and development of the so-called 'conducting polymers'. The award was received giving the following Nobel Lectures: The discovery of polyacetylene film: The dawning of an era of conducting polymers (Nobel Lecture) by Shirakawa (2001); 'Synthetic metals': A novel role for organic polymers (Nobel Lecture) by MacDiarmid (2001); semi-conducting and metallic polymers: The fourth generation of polymeric materials (Nobel Lecture) by Heeger (2001).

b. Polyaniline

Among the conducting polymers, polyaniline (PAni) is emerging as the material of choice for many applications. Aniline, the monomer of the polynailine, was first obtained in 1826 from the pyrolytic distillation of indigo and was found to produce crystallline salts with sulphuric and phosphoric acid (Wise *et al.* 1998). Fritsche (1840) isolated colorless oil from indigo and oxidized to PAni (Fritsche, 1840). Lethebey (1862) reported the electrochemical synthesis of PAni when he observed the growth of a blue-green powdery pigment on a platinium anode during the electrolysis of a solution of aniline in sulphuric acid. Lethebey's findings were verified in nineteenth century investigators, and

the pigment was named “aniline black”. The oxidation of aniline in hydrochloric acid was found to produce a similar product and conductivity of this product was reported by Green and Woodhead at 1910 (Wise *et al.* , 1950). Letheby’s original observations and findings were confirmed again by Khumotov and Gorbachev in 1950’s (Wise *et al.* , 1998).

Mohilner *et al.* , (1962) investigated the kinetics of electrochemical oxidation of aniline in sulphuric acid and deduced that the initial oxidation requires the formation of aniline radical as shown in Figure 1 (Wise *et al. ,* 1998):

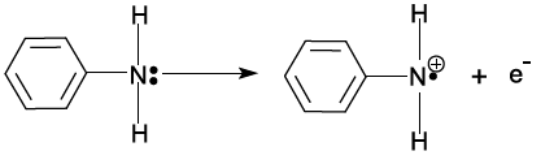

Figure 1. Formation of aniline radical

Mohilner *et al.* , (1962) synthesized the aniline chemically to conclude that the oxidation states of aniline in two basic conversion leucoemeraldine base to emeraldine salt, from emeraldine salt to pernigraniline salt. Emeraldine salt is reported as dark green salt. Chiang and MacDiarmid (1986) proposed representation of conversion of PAni from insulator form to the conductor form by oxidation and reduction as illustrated in Figure 2:

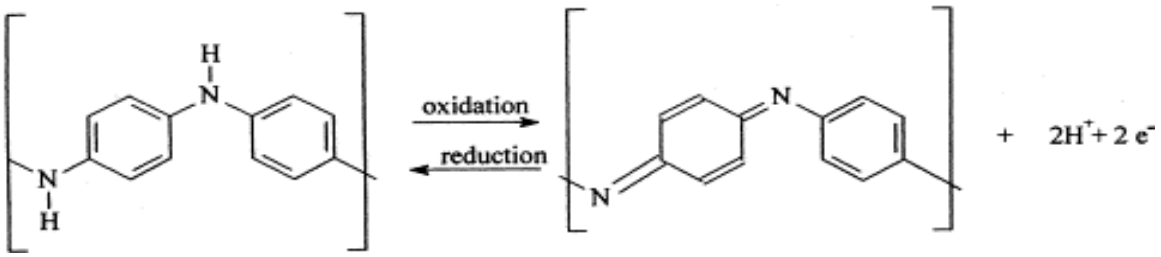

Figure 2. Representation of polyaniline: from insulator to conductor by oxidation; from conductor to insulator by reduction.

PAni is typically prepared by the chemical oxidation of aniline or anilinium salts, such as aniline hydrochloride or aniline sulfate, in acidic aqueous medium. Ammonium peroxydisulfate (APS) being the most common oxidant (Stejskal *et al.* 2002; Gospodinova *et al.* , 1998). Emulsion polymerization route also has been adopted to prepare processible conducting PAni, wherein aniline was polymerized in an emulsion of water and a non-polar or weakly polar organic solvent in the presence of dodecylbenzenesulfonic acid (DBSA) (Österholm *et al.* , 1993 and Österholm *et al.* 1994). Kinlen *et al.* (1998) have followed a slightly different route in emulsion polymerization pathway to prepare PAni salt; i. e. , aniline was oxidized by ammonium persulfate in water, water miscible solvent (2-butoxyethanol) using water-insoluble organic acid (i. e. , dinonylnaphthalenesulfonic acid).

Kinlen *et al.* (1999) obtained soluble ABA triblock polymers (where A—PAni, B—diamine terminated derivative of polyethyleneoxide, or polypropylene oxide or polydimethylsiloxane or polyacrylonitrile-*co*-butadiene) by emulsion polymerization

pathway. Stejskal *et al.* (2002) prepared conducting PAni with the project group at different laboratories. The project has been inspired by an occasionally expressed opinion that “there are as many polyaniline as the number of people who prepare them”, and attempting to check whether to what extent this hypotheses is true. Synthesis was based on mixing aqueous solutions of aniline hydrochloride and ammonium peroxydisulfate at room temperature by oxidation pathway polymerization. Standard polymerizations of aniline have been made by eight individuals from five institutions in five different countries. PAni powders were collected from all the participants at the Institute of Macromolecular Chemistry in Prague, compressed into pellets and subjected to determination of conductivity. The average conductivity was 4. 37 S cm^{-1}. Savitha *et al.* (2004) reported their finding on synthesis of conducting copolymer poly(aniline-*co*-aminoacetophenone) by emulsion and inverted emulsion methods. By changing the molar feed ratio of aniline and *o*/*m*-aminoacetophenone, different compositions of copolymers have been synthesized. Conductivity values of the copolymers were found to be nearly the same and they varied from 1. 6 to 3. 0×10^{-2} S cm^{-1}. Wang *et al.* (2006) studied on a novel Zn-PAni dry rechargeable battery. Conducting PAni powder was well mixed with graphite and acetylene black to obtain the optimum conductivity and porosity.

Kim *et al.* (2007) reported the synthesis procedure of organic soluble PAni preparation by one-step emulsion polymerization pathway, which was carried out in toluene / water solvent system. DBSA was used as the surfactant and acid and APS was used as the oxidant. At the end of the reaction, the toluene layer was separated and analyzed. PAni

film was prepared from PAni solution by either spin coating or roll coating method. Conductivity and transmittance were 2–4×10^{-1} S cm^{-1} and >75% for <550 nm thick films, and 1 S cm^{-1} and 30% for <1 μm thick films. AFM image of PAni film with less than 500 nm thickness shows very homogeneous surface structure and very dense membrane, which suggested that undissolved particles may not be present in PAni solution. Stejskal *et al.* (2008) studied on reprotonation of polyaniline. PAni base was immersed in aqueous solutions of 42 inorganic or organic acids in order to find out, which was able to constitute a salt with the PAni base and what are the properties of products. The conductivity of the reprotonated PAni bases was determined especially by the pH of acid solutions. The highest conductivity, 1. 22 S cm^{-1} was found after reprotonation of PAni base with 50% tetrafluoroboric acid. The reaction with most strong inorganic acids yielded samples with a conductivity of 10^{-1} S cm^{-1}. Sulfonic acids gave products having conductivity of the order of 10^{-2}–10^{-1} S cm^{-1}. Carboxylic acids were less efficient in protonation, and their ability to produce a conducting polymer depended on increasing the acid concentration. Acids containing an acidic hydroxyl group, like picric acid, also protonated PAni to a good level of conductivity. The lowest conductivity, 1. 8 × 10^{-10} S cm^{-1} was observed in the absence of any acid.

Most recently Wanga *et al.* (2009) synthesized electrically conductive core–shell nanoparticles (PAni / PS-PSS) by coating poly (styrene-co-styrene sulfonate) (PS-PSS) nanoparticles with PAni. PS-PSS core particles were prepared in microemulsion system in nitrogen atmosphere and further coated with PAni by using in situ polymerization method at low temperature. The core–shell structure of PAni / PS-PSS composites was

determined by transmission electron microscopy (TEM) and FTIR measurements. In addition, the role of the aniline content was also investigated. The stability of the coated latexes and the conductivity of PAni / PS-PSS pellets were investigated. It was found that the core–shell structure of PAni-coated PS-PSS can be obtained when PAni in PAni / PS-PSS copolymer varies from 2. 78 to 12. 5wt%. The highest conductivity of PAni / PS-PSS pellets was 1. 7 S cm^{-1}. Many reviews about preparation of polyaniline have been published. Bhadra *et al.* (2009) reviewed all the synthesis, processing and applications of PAni; this study included the advantages of the intrinsically conducting polymers (ICPs) over the other conducting polymers and the superiority of PAni among other ICPs. Details are provided of the different methods used for the synthesis of PAni along with a number of special methods used to obtain a nanostructured PAni. A detailed discussion on the mechanism of electrical conduction in PAni and the factors that influence the conductivity of PAni were also included. Dhand *et al.* 2011 rewied all the biosensing applications of the PAni.

c. Graphene

Carbon nanotubes were major area of materials research until the discovery of the graphene by Andre Geim *et al.* , Manchester University, United Kingdom in 2004. Although previous attempts to produce graphene had been tried before, they were not successful. Andre Geim thought it might be possible to do something similar to carbon nanotubes, only in an unfolded configuration. He had the idea to polish down a graphite block to just 10 or 100 layers thick and then study the material's properties. One of his students was assigned the task, and produced a speck of graphite roughly 1000 layers

thick–a little short of the mark. That is when Geim had the idea to use Scotch tape to peel away the top layer. Flakes of graphite come off onto the tape, and the process can be repeated several times to achieve progressively thinner flakes attached to the tape. He then dissolved the tape in solution, leaving him with ultra-thin flakes of graphite: just 10 layers thick. Within weeks, his team had begun fabricating rudimentar y transistors with the material. Subsequent refinements of the technique finally yielded the first graphene sheets. “We fooled nature by first making a three-dimensional material, which is graphite, and then pulling an individual layer out of it, said Geim.

In fact, before graphene isolating, the experimental evidence of existence of the single-nano graphene has been reported in 2001, by Affoune *et al.* In this study was reported that, it is possible to observe graphene sheets 0. 35-0. 37 nm interlayer distance, by Atomic Force Microscopy. After the achievement of graphene sheets in *Science* magazine, the studies were continued to know about this novel material. And in many articles has been reported that, graphene is a more one atom thick– perhaps the thinnest material in the universe–and forms a high-quality crystal lattice, with no vacancies or dislocations in the structure. This structure gives it intriguing properties, and yielded surprising new physics. The article entitled “Electric field effect in atomically thin carbon films” is now one of the most highly cited papers in materials physics, and in 2005, by researchers who had succeeded in isolating graphene sheets. But we have to know that also before the experimental discovery of the graphene, the distinct nature of charge carriers in a hexagonal carbon lattice has been speculated upon and was

proposed to have important implications on the electronic transport in graphitic materials by Novoselov *et al.* (2004).

The second exciting report, after the isolating the graphene was the discovery of field effect of graphene by Manchester Group. Novoselov *et al.* , (2004) reported the observation of the electric field effect in a naturally occurring two dimensional (2D) material referred to as few-layer graphene (FLG). They processed the films into multiterminal Hall bar devices placed on top of an oxidized Si substrate so that a gate voltage (Vg) could be applied. They have studied more than 60 devices with d<10 nm. They focus on the electronic properties of our thinnest (FLG) devices, which contained just one, two, or three atomic layers. All FLG devices exhibited essentially identical electronic properties characteristic for a 2D semimetal, which differed from a more complex behavior observed for thicker, multilayer graphene as well as from the properties of 3D graphite. The observed behavior resembles the ambipolar field effect in semiconductors, but there is no zero-conductance region associated with the Fermi level being pinned inside the band gap. It has been reported measurements can be explained quantitatively by a model of a 2D metal with a small overlap between conductance and valence bands. One of the important points which has been reported, is that Hall resistivity results served as an indicator of the quality and homogeneity of the graphene, and also reported the agreement with the fact that the single layer graphene is in theory a zero-gap semiconductor.

After the discovery of the graphene, various attempts were made to synthesize graphene, graphene oxide, and functionalized graphene. Niyogi *et al.* (2006) and Stankovich *et al.* (2006) used ultrasonic dispersions to obtain functionalized graphene. Exfoliation of graphite oxidized with strong acids either by rapid thermal expansion has been worked by Schniepp *et al.* (2006). Si and Samulski (2008) synthesize water-soluble graphene by sulfonation of graphene oxide. The results indicate that the bulk of the oxygen-containing functional groups were removed from graphene oxide; the electrical conductivity of thin evaporated films of graphene was of 1250 S cm^{-1}. Similarly, Li *et al.* (2008) worked on aqueous dispersion of graphene.

The chemical structure of the graphene oxide, because of its basal plane is decorated with hydroxyl and epoxy, suggested such a variety of surface-modification reactions to develop the functionalized graphene oxide- and graphene-based materials. Many works have reported on the chemical reduction of graphene oxide (Stankovich *et al.* , 2007; Eda *et al.* , 2008; Becerril *et al.* , 2008 and Ramanathan *et al.* , 2008; Zhu *et al.* 2009) reported the synthesis of readily soluble graphene in organic solvents such as N,N-dimethylformamide and N-methyl-2-pyrrolidinone using diazonium salt functionalization. Lately, synthesis of few layer graphene sheets using chemical vapor deposition method have been widely investigated by Malesevic et al, (2008), Vitchev *et al.* (2010), and Lee *et al.* (2010).

Most recently, Chen *et al.* (2011) prepared the sulfonic functionalized graphene oxide, by some sulfonation routes, for instance, through amide formation between the

carboxylic group of GO, and amine of sulfanilic acid (AA–GO–SO_3^-). Zhao *et al.* (2011) also worked on sulfonated graphene. They reported that sulfonated graphene in aqueous solution is capable of absorbing aromatic pullutants from aqueous solutions.

d. PAni / Graphene composites

The studies based on polyaniline and graphite started in 2003. In 2004, it was reported the fabrication and characterization of novel, monolithic electrochemical actuators, based on PAni and a micrometer-sized graphite powder by Li *et al.* They reported that these PAni–graphite thin films have a graphite-rich layer that renders composite thin film conductive at all redox states. In 2004 also, a facile process for the synthesis of exfoliated graphite and polyaniline / graphite nanocomposite was developed by Du *et al.* Graphite nanosheets were prepared via the microwave irradiation and sonication from synthesized expandable graphite. The nanocomposites were fabricated via *in situ* polymerization of aniline monomer in the presence of graphite nanosheets. According to the results, electrical conductivity measurements indicated that the conductivity of final PAni / graphite nanocomposites increased greatly compared with pure PAni. The conductivity of the nanocomposite with only 1. 5wt% graphite nanosheet was 33. 3 S cm^{-1}, which was six times greater than that of neat PAni (about 5 S cm^{-1}).

Bourdo and Viswanathan (2005) studied the synthesis and characterization of graphite / polyaniline composites. They found that the exploration of graphite / PAni composites yielded conducting composites which exhibited conductivities greater than the graphite

or PAni alone. Lately, in 2007, the characteristics of polyaniline / graphite composites were studied in aqueous electrolyte. The PAni / graphite films, with different graphite particle sizes were deposited on a platinum electrode by Ghanbari *et al.* to make batteries. To compare two types of batteries were fabricated: Zn-PAni / graphite and Zn-PAni. Studies on the Zn-PAni / graphite cell clearly demonstrated the viability of using this composite as an active electrode material. The Zn-PAni / graphite batteries, according to the number of key factors such as capacity, columbic efficiency and specific energy were improved compared to other works, and the performance of the cell was found to be better than that of the Zn-PAni battery.

More lately, Wang *et al.* (2009) studied the synthesis of graphene oxide doped polyaniline for supercapacitors. It has been reported that a novel high-performance electrode material based on fibrillar polyaniline (PAni) doped with graphene oxide sheets was synthesized via in situ polymerization of monomer in the presence of graphene oxide, with a high conductivity of 10 S cm^{-1} at 22°C for the obtained nanocomposite, with a mass ratio of aniline / graphite oxide, 100:1. Zhao *et al. ,* (2009) prepared transparent, conductive and uniform graphene used them as electrodes of the electrochromic devices of polyaniline. It was reported that PANI was synthesized by chemical oxidation of aniline with ammonium persulfate at 0°C. An aqueous dispersion of GO was produced by the Hummers' method, and purified through dialysis and centrifugation. The GO sheets were deposited on pretreated hydrophilic quartz substrates by the dip-coating method for preparing the electrodes. PAni was spincoated onto graphene electrodes to fabricate electrochromic electrodes, named as PAni-

graphite electrodes. To compare also PAni spincoated onto ITO slides, the electrodes were characterized by CV for electrochemical activities, and by Spectroelectrochemistry for optical properties. According to the results, the performances of the electrochromic devices with graphene electrodes exhibited slight decrease upon voltage switching, while those of the devices with ITO electrodes decreased dramatically. After 300 cycles, the electrochromic devices with graphene electrodes showed much larger optical contrast, and shorter switching time than those of the devices with ITO electrodes.

More recently, graphene nanosheet (GNS) / PAni composite was synthesized using *in situ* polymerization by Yan *et al.* (2010). According to the results, the GNS / PAni composite exhibited more electrochemical active sites compare to the graphene and PAni itself. Yang (2010) studied graphene nanosheet / carbon nanotube / polyaniline (GNS / CNT / PAni) composite. It was reported that the CNTs used as conductive wires between GNS and PAni particles, produced highly conductive composites.

To exploit the potential and to enhance the electrical conductivity, PAni / graphene based materials have been prepared via different synthesis. Wang *et al. ,* (2009) prepared graphene / polyaniline composite by *in situ* anodic electropolymerization of aniline on graphene paper. Firstly, graphene paper on cellulose membrane was obtained by vacuum infiltration of graphene suspension, then aniline was electropolymerized on the graphene paper by *in situ* anodic electropolymerization to form PAni. This composite paper combines flexibility, conductivity, electrochemical

activity, and exhibits gravimetric capacitance of 233 F g^{-1}. Zhang *et al.* , (2010) synthesized chemically modified graphene and polyaniline nanofiber composites by *in situ* polymerization of aniline monomer in the presence of graphene oxide. The obtained graphene oxide / PAni composites were reduced to graphene using hydrazine followed by reoxidation and reprotonation of the reduced PAni to give the graphene / PANI nanocomposites. The specific capacity of the material was recorded as 480 F g^{-1}. Wang *et al.* (2010) also prepared graphene / PAni hybrid material as a supercapacitor electrode. The composite was synthesized by three-step *in situ* polymerization; the first step, started by the synthesis of graphene oxide / PAni composite through *in situ* polymerization; in the second step, graphene oxide was reduced. and in the third step, PAni was dedopped. A high specific capacitance of 1126 F g^{-1} was obtained. More recently, Hao *et al.* (2010) fabricated sulfonated graphene / polyaniline nanocomposites by liquid / liquid interfacial polymerization. In the fabrication process firstly, graphene oxide was reduced and treated by diazonium salt of sulfanilic acid to form sulfonated graphene (SGr). An aqueous mixture of sulfonated graphene as the water phase and aniline in chloroform as the oil phase were used to synthesis SGr / PAni composites through interfacial polymerization. Lately, Feng *et al.* (2011) explored the new one-step synthesize to obtain PAni / graphene composites by electrochemical synthesis by using GO and aniline as the starting materials. The aniline monomer and GO were first mixed, and then casted onto ITO. CV was run, and aniline monomer was oxidized and polymerized on the surface of GO and GO was reduced to graphene at the same time. Furthermore, the composite was directly used as the supercapacitor electrode. This supercapacitor showed a high specific capacitance of 640 F g^{-1}.

III. JUSTIFICATION

Since the first report on the isolation of graphene, it has become a top area of research in materials science. Nowadays, graphene is one the most attractive nanomaterials because of its excellent electrical, thermal, optical properties. It has also been reported that it is the thinnest known material and the strongest ever measured. On the other hand, because of its environmentally stability, low cost of raw materials and ease to synthesis, PAni is the most intensively investigated intrinsically conducting polymer. Its electrically conductive form is found to be difficult to process; thus, in order to diversify these difficulties PAni can be mixed with other materials to obtain new composites with novel properties. Therefore, the nanocomposites of the PAni / graphene are expected to have improved conductivity and increased electroactivity. As a result, the present study pretends to contribute to the exhaustive investigations of electrically conductive polymers performed in the last years. Besides, it will also contribute to open the niche to fabricate new PAni / graphene nanocomposites for sensor, or capacitor devices. It is expected that this work will serve as a motivation of further studies for keeping on finding out different methods to functionalize graphene with electrically conductive polymers, to develop new types of electroactive materials.

IV. HYPOTHESES

Through the incorporating technique of graphene oxide to leucoemeraldine salt of polyaniline, we would be dopping the polyaniline while reducing the graphene oxide to graphene, thanks to the oxygen functionalities on the surface of the graphene

oxide. This technique makes easy the synthesis of PAni / graphene composites because of no longer reduction step is required. By this technique, we would be dopping the polyaniline by functionalized graphene. Consequently, the PAni / graphene composites will show both improved electrical conductivity and high electroactivity. In addition, it is expected that this materials show capacitance property**.**

V. OBJECTIVE

Developing the methodology to synthesize electroactive and highly electrical conductive composites based on PAni and Graphene.

Particular Objectives

- Developing a reproducible method to modify graphite to graphene oxide using the Hummer´s method.
- Characterization of the physical properties of the graphene nanosheets and modified graphene via infrared and Raman spectroscopy.
- Synthesize of leucoemeraldine salt of polyaniline.
- Synthesize polyaniline / graphene composites through:
    - Incorporation of graphene oxide, as the doping agent, to leucoemeraldine salt of PAni.

    - In situ polymerization of polyaniline in the presence of the sufonated graphene.

- Characterization of the physical properties of the polyaniline / graphene composites through infrared spectroscopy, UV-vis spectroscopy, cyclic voltammetry, and conductivity measurements through the four-probe method.

CHAPTER II

VI. THEORITICAL ASPECTS

POLYANILINE

The polyanilines are a class of organic polymers with an alternating ring –heteroatom backbone structure. A wide variety of derivates can be synthesized by the substitution on the benzene ring, or on the nitrogen atom. It can exist in at least six different forms, both salt and base versions of leucoemeraldine, emeraldine and pernigraniline. Leucoemeraldine is fully oxidized, emeraldine is half-oxidized and half-reduced, and pernigraniline is fully reduced. Figure 3 illustrates the chemical structures of four oxidation states of polyaniline (Wallace *et al.* 2002). The production of polyaniline fibers would be rather simple if processing could be achieved with the most desired oxidation state, emeraldine salt (PAni-ES). However, the insolubility of PAni-ES, the only conductive form of polyaniline, requires an alternative approach to processing. Hence, the total process involves the conversion of emeraldine base to leucoemeraldine base and eventually to emeraldine salt. This procedure will be explained in detail when discussing the synthesis.

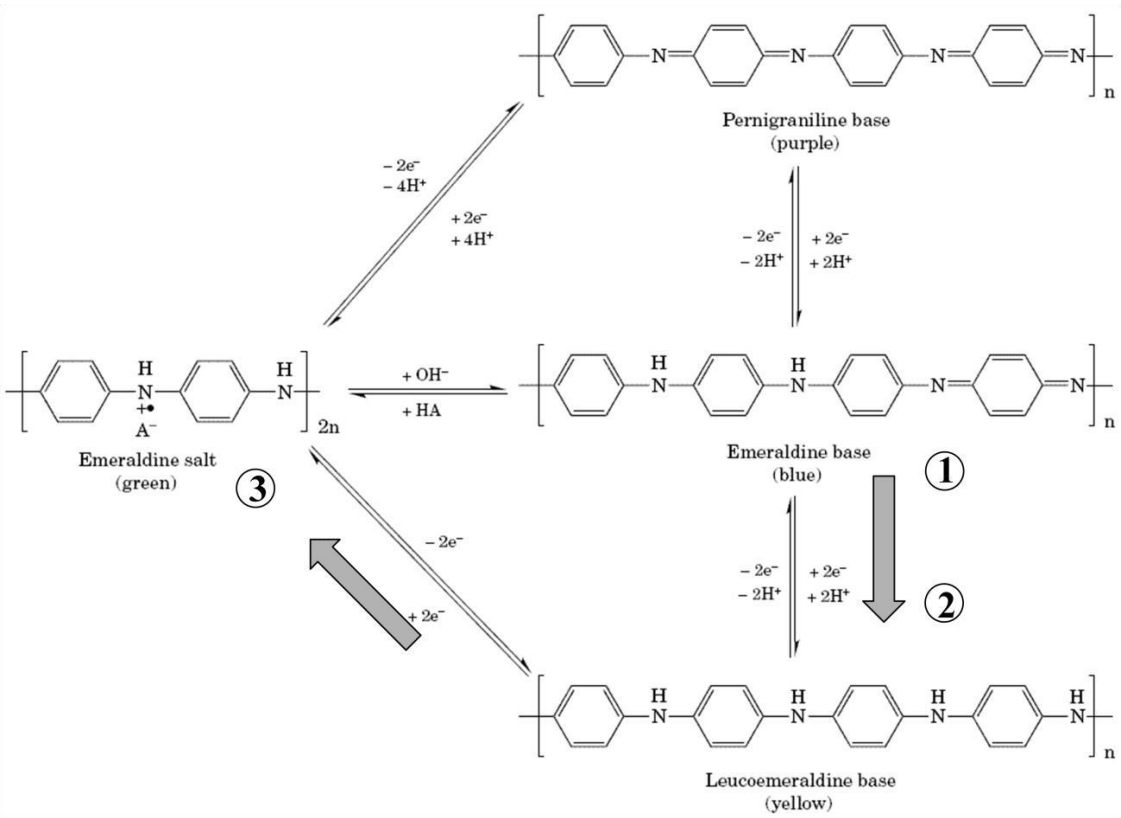

Figure 3. Conversion mechanism of polyaniline

Polyaniline Synthesis

The conventional synthesis of polyaniline and its morphology has been given in the Figure 4. The oxidative polymerization reaction of aniline is typically carried out in an acidic solution (e. g. , 1 M HCl). The prepared polyaniline is in its doped emeraldine form, which can be de-doped by a base to its emeraldine base form.

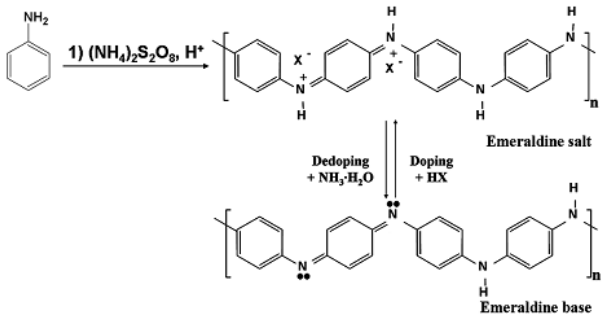

Figure 4. The conventional synthesis of polyaniline

The doping mechanism of polyaniline and the conductivity

In polyaniline, protonic acid doping involves the addition of protons to the polymer backbone. The resulting positive charge is balanced by negatively charged anions transferred from the doping agent, which is an aqueous and acidic solution. Protonation also introduces a delocalization of a radical cation, termed a polaron. A polaron is essentially a charge carrier with a surrounding field of polarization. An increase in doping levels is accompanied by the formation of a bipolaron, which is a pair of polarons. This formation reduces the aforementioned band gap between the valence band and the conduction band, making actuation possible (Bredas *et al.* 1984). In polyaniline, optimum level of doping are accompanied with an increase in conductivity. Therefore, the PAni must be subjected to doping in order to achieve conducting forms.

GRAPHENE

In 1859, the British chemist B. C. Brodie explored the structure of graphite and the reactivity of flake of graphite. Throughout his studies, Brodie was interested in the

molecular formula of ‘‘graphite’’ and its discrete molecular weight. Ultimately, he determined the molecular weight of graphite to be 33, saying:

‘‘This form of carbon should be characterized by a name marking it as a distinct element. I propose to term it Graphon. ’’

Nearly 150 years later, ‘‘graphene’’ would take the physics and chemistry communities by storm.

Structural Features

Graphene is a single layer of carbon atoms tightly packed into a two-dimensional honeycomb lattice. Graphene is part of the family of atomic "nano-carbons" that includes diamond, carbon nanotubes, buckeyballs (C60 fullerenes), and is a single or a few atomic layers of the three-dimensional material graphite. In these materials, carbon bonds are bonded in different manner. In diamond each atom is bonded tetrahedrally, in fullerenes carbon atoms bend the sheet into spheres, ellipses, or cylinders. The buckyballs are large molecules formed completely of carbon bonded trigonally; carbon nanotubes are structurally similar to buckyballs, except that each atom is bonded trigonally in a curved sheet that forms a hollow cylinder (Figure. 5)**.** Graphite has a layered, planar structure. In each layer, the carbon atoms are arranged in a hexagonal lattice (Figure. 6)**.**

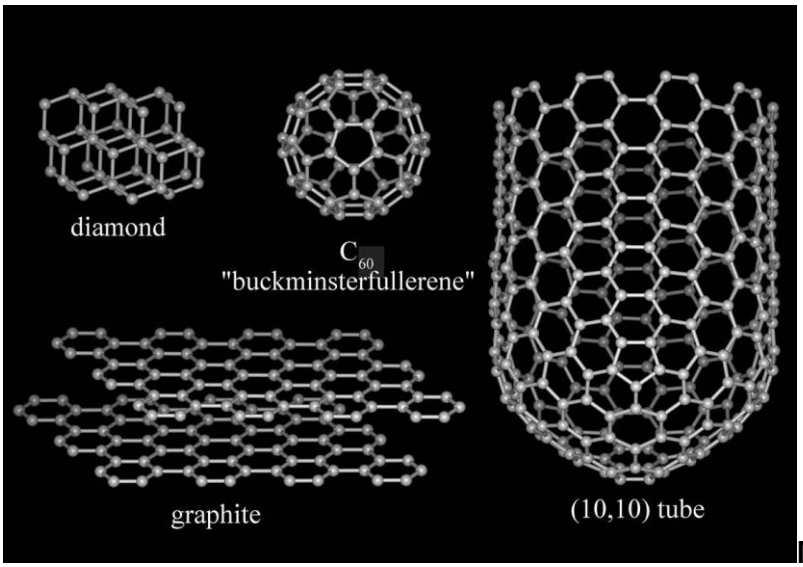

M

Figure 5: All graphitic forms

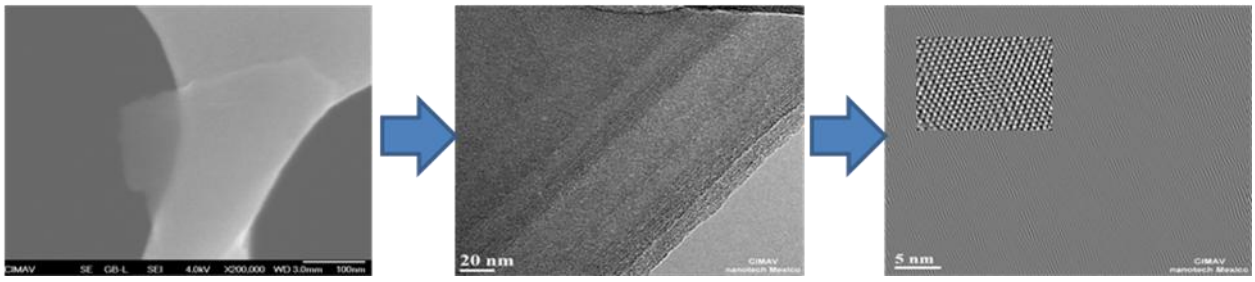

Figure 6: TEM images and hexagonal atomic arrangement of graphene nanosheets

Conductivity in Graphene

Graphite can conduct electricity because of the vast electron delocalization within the carbon layers (a phenomenon called aromaticity). These valence electrons are free to move (Figure. 7), so are able to conduct electricity (Zhu *et al.* , 2010). However, the electricity is primarily conducted within the plane of the layers. Thus, at the moment graphene is the most widely studied carbon based material for its remarkable electronic transport properties (Singh *et al.* , 2011).

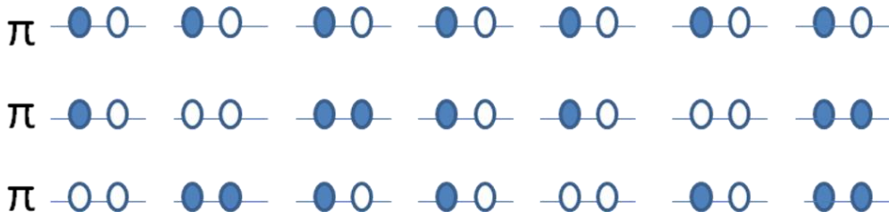

Figure 7. Electron hopping mechanism in valence electrons of graphene

From graphite to graphite oxide, from graphite oxide to graphene

In recent years, various synthetic approaches have been pursued to prepare graphene nanosheets. Among the various strategies pursued, the reduction of graphite oxide (GO) is one of the most promising methods (Tung *et al.* , 2009). Graphite oxide, formerly called graphitic oxide is a compound of carbon, oxygen, and hydrogen in variable ratios, obtained by treating graphite with strong oxidizers (Dreyer *et al.* , 2010). The mechanism of graphite oxide by oxidizers is mainly the generation of oxygen-containing groups on the graphene sheets as seen in the Figure 8 and 9.

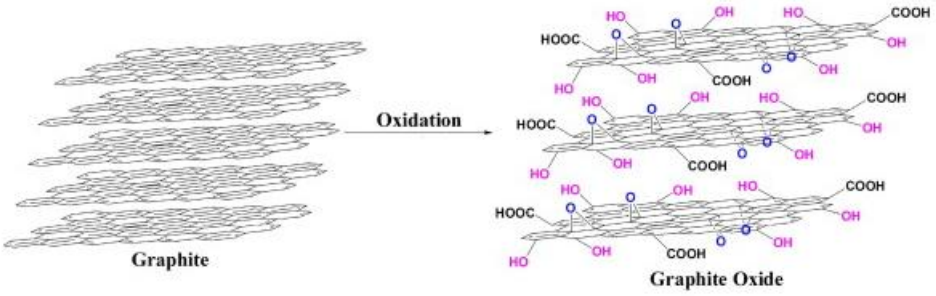

Figure 8. Graphite oxidation

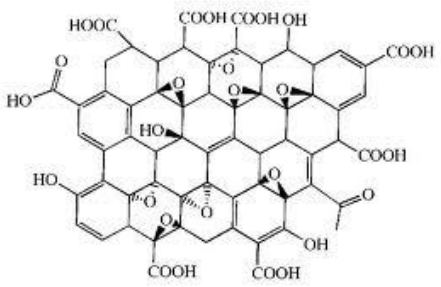

Figure 9. Oxidized graphite

Graphite oxide contains oxygen functionalities but remains stack structured, similar to graphite with much wider spacing due to water intercalation. Graphite oxide reduction was probably historically the first method of graphene synthesis. Reduction as known is decrease in oxidation state. So, a reducing agent is used to reduce / eliminate the oxygen-containing group on the graphene sheets. The reducing agents creates basic media, which weaken the platelet–platelet interaction owing to its hydrophilicity (Dreyer *et al.* , 2010)

Reduction is realized by most of the time with reducing agents, heating, and ultrasonication. In graphene, rather than retaining a stacked structure, the material is exfoliated into monolayers or few-layered structure due to greatly weakening of the surface functionality between layers. Reduction of graphite oxide monolayer films e. g. by hydrazine (Figure. 8), annealing in argon / hydrogen, sodium hydrite, hydrochinone, p-phenylene diamine, strongly alkaline solution, supercritical water, H_2-plasma, electrochemical reduction was reported to yield graphene films (Eda and Chhowalla, 2010). However, the quality of graphene produced by graphite oxide reduction is lower

compared to e. g. scotch-tape graphene due to incomplete removal of various functional groups by existing reduction methods.

Functionalization of Graphene

The recent advancement in bulk synthesis processes of graphene oxide and reduced graphene oxide has generated great interest to incorporate such unique material into various polymer matrices. Several challenges need to be overcome to realize graphene or graphene oxide based polymer composites e. g. functionalization of graphene sheets, homogeneous dispersion of materials with minimal restacking, effective mixing of graphene oxide and graphene with polymer.

Taking into account that GO has carboxylic, hydroxyl and epoxy groups on the surface, which improve its dispersion in water, and keep individual layers separated from each other (Figure 10), the functional groups introduced to graphene, can be used to achieve good dispersion of derived graphene in different solvents. Numerous efforts have been made to improve the dispersion of GO and RGO by functionalizing the use of organic molecules compatible with the polymer matrix to enhance interfacial interaction with the matrix (Stankovich *et al.* , 2007).

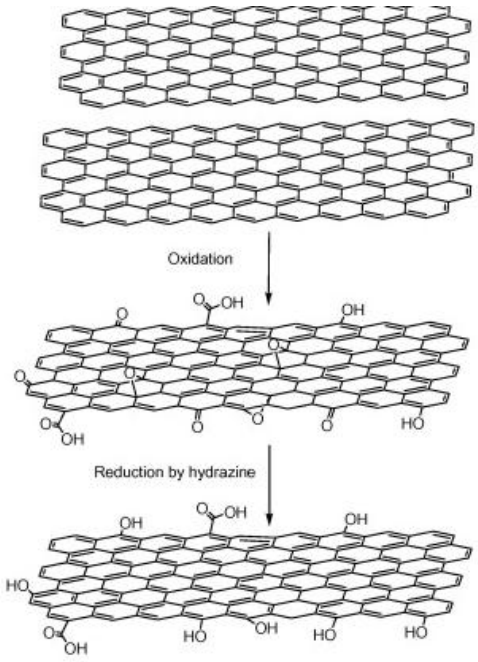

Figure 10. Reducing graphene by hydrazine

POLYMER / GRAPHENE COMPOSITION

In this work, two types of polymer / graphene composites are reported.

According to the first method, simultaneous reduction of graphene oxide occurs while simultaneous oxidation of polyaniline is occurring (Figure. 11). This donor-acceptor interaction between the leucoemeraldine salt of polyaniline and graphene oxide can be explained by charge transfer between materials (Vallés *et al.* , 2011). The synthesis mechanism exhibits an unprecedented donor–acceptor interaction at the interface between GO sheets and the leucoemeraldine state of polyaniline. A conceptual explanation is proposed in which GO plays a dual role as electron acceptor and as large counterion for polyaniline.

According to the second method, the modified graphene sheets, was incorporated into the PAni matrix during the *in situ* polymerization synthesis of the PAni / graphene composites as seen in the Figure 12.

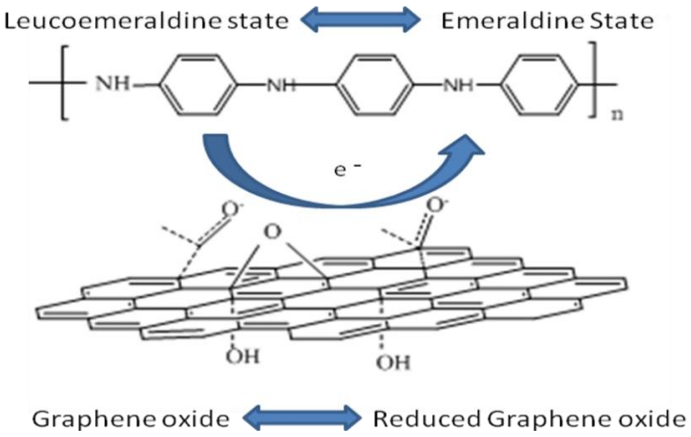

Figure 11. Simultaneous oxidation of polyaniline

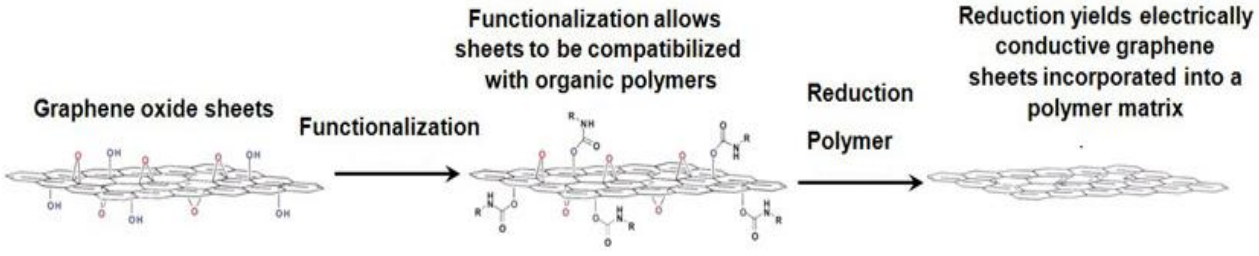

Figure 12. Incorporation of the sulfonated graphene onto PAni

VII. EXPERIMENTAL SECTION

Materials

GO was synthesized from natural graphite powder (Sigma-Aldrich) via Hummers-Offeman method by sulfuric acid (H_2SO_4, 99%, Panreac), potassium permanganate ($KMnO_4$, Panreac), hydrogen peroxide (H_2O_2, Panreac) and sodium nitrate ($NaNO_3$, Sigma-Aldrich). GO reduced by hydrazine (N_2H_4, Aldrich Co.) Sulfonated graphenes were synthesized by sulfanilic acid (99%, Sigma-Aldrich), amino-4-hydroxy-2-naphthalenesulfonic acid (99%, Fluka) and isopentyl nitrite (Sigma-Aldrich). Aniline (Sigma-Aldrich) was purified by distillation under reduced pressure prior to use. Polyaniline is polymerized by HCl (37%, Analar NORMAPUR) and ammonium persulfate (APS, Sigma-Aldrich). Buffer solutions were prepared by potassium dihydrogen phosphate (KH_2PO_4, Sigma-Aldrich), acetic acid (CH_3COOH, Jaber Ind.), and sodium acetate (CH3COONa, Aldrich) and sodium chloride (NaCl, Scharlau).

Experimentation

General procedure for the synthesis of graphite oxide by Hummer´s method:

The graphite oxide was synthesized from powder graphite by the fallowing procedure (Hummer´s method): 10 g of natural graphite flake powder was mixed with 5 g sodium nitrate in 0. 2 L of H_2SO_4. The mixture was cooled to 0^0C in an ice bath, while stirring 30 g of $KMNO_4$ was added to the suspension gradually to avoid the temperature exceeding 20°C. The ice bath was removed, and 0. 4 L of distilled water were added

slowly to the mixture, which results in effervescence and an increase in temperature to 98^0C. The brown colored suspension was maintained at this temperature for 15 min. The suspension was diluted to 1. 4 L of 3% H_2O_2 in warm water, followed by filtration and washing using 1 L of H_2O. The filtered cake was dried by vacuum to use in further process and stored until needed for experimentation.

Method 1:

General procedure for the synthesis of emeraldine salt of PAni

In this procedure, 9. 3 mL of aniline was dissolved in a 1 M HCl / water solution (80 mL). The solution was cooled to 0-5ºC in an ice bath, and the oxidant, ammonium peroxydisulfate, $(NH_2)_4S_2O_8$, 5. 7 g in 20 mL) was added to launch polymerization. The polymerization was left to occur under vigorous stirring at 0°C for 3 h. The product was filtered and washed with water, followed by drying under vacuum.

Synthesis of chemically reduced PANI (leucoemeraldine salt of PAni):

Here, 1 g of PAni was dispersed in 100 mL, 1 M solution of NH_3. The dispersion was stirred under nitrogen atmosphere for 96 h. Then filtered and washed several times by deoxygenated distilled water by vacuum.

Synthesis of PAni / reduce GO (RGO)

The GO obtained by the Hummer´s method was dispersed in distilled water at a concentration of 50 mL / mg. Chemically reduced PAni (leucoemeraldine state) was added to the GO dispersion. The mixture was heated at 60°C for 3 h and mixed by magnetic stirring for 24 h. After this time, the material was filtered and washed several times. The solid was left to dry. The PAni / GO composites were prepared by different mass ratios: 75:10, 75:20, 75:30, or 75:50, and resulting composites were respectively named as PAni / RGO 100, PAni / RGO 200, PAni / RGO 300, and PAni / RGO 500.

Preparation of PAni / GO composites

For comparison purposed, composites of PAni / GO were prepared by *in situ* polymerization of aniline in a graphite oxide dispersion. First, 2 g of graphite oxide was dissolved in 100 mL of distilled water and sonicated for 30 min. Next, 9. 3 mL of aniline and 9. 87 mL of HCl were added and mixed vigorously. The dispersion was cooled to 0-5ºC in an ice bath and ammonium peroxydisulfate (5. 7 g) was added to launch the polymerization. The mixture has allowed stirring at room temperature overnight. The composite was collected by filtration and washed several times by distilled water, 0. 1 M ammonium solution and finally with a 1 M HCl solution. The composite was dried at 60^{o}C in a vacuum oven

Method 2.

Preparation of sulfonated graphene (SGrf).

GO (1 g) was dispersed in 250 mL of ultrapure water in a round-bottomed flask and then, sonicated for 30 min. Next, 5 mL of 50% hydrazine solution was loaded and heated to 90ºC for 3 h. The material was filtered and washed repeatedly with water. The solid was dissolved in 250 mL of buffered solution at pH 8 to avoid precipitation, and 5. 04 g of sulfanilic acid and 3 mL of isopentyl nitrite were subsequently added. The reaction flask was kept at 80ºC under magnetic stirring overnight. After cooling at room temperature, the product, called as GSA was filtered, and washed with abundant water. The procedure was repeated for the sulfonation with amino-4-hydroxy-2-naphthalenesulfonic acid (6. 97 g) and the product was called as GNSA.

Synthesis of PAni/ sulfonated graphene (PAni/ SGrf)

The composites were prepared by polymerization of aniline in a solution containing dispersed SG. Briefly, 0. 1 g of GSA was dispersed in 100 mL of water and treated with ultrasound for 20 min. Then, 9 mL of HCl and 9. 3 mL of aniline were added. The dispersion was cooled to 0-5ºC in an ice bath and ammonium peroxydisulfate (5. 7 g) was added to launch the polymerization. The polymerization was left to occur under vigorous stirring at 0ºC for 3 h. The product, called as GSA / PAni was filtered and washed with water, followed by drying under vacuum. The same procedure was employed for the preparation of PAni and GNSA and the material was called as PAni / GNSA

VIII. CHARACTERIZATION

INFRARED SPECTROSCOPY

An infrared spectrophotometer (Spectrum One FTIR, Perkin Elmer) was used to collect spectras in transmission mode at a resolution of 4 cm^{-1}. The samples of the synthesized materials were prepared in pellets with potassium bromide (KBr).

UV-VIS SPECTROSCOPY

An UV-VIS spectrophotometer (Spectrum One FTIR, Perkin Elmer) was used to collect spectras in absorption mode from 200 to 700 nm. The powder materials were dissolved in NMP solution (1 mg/1 mL).

RAMAN SPECTROSCOPY

A Raman system (InVia Raman microscope, Renishaw) was used, employing a grating spectrometer with a Peltier-cooled charge-coupled device (CCD) detector coupled to a confocal microscope. All spectra were processed using the Renishaw WiRE 3. 2 software. The Raman scattering was excited using an Argon ion laser with wavelength of 514. 5 nm. The laser beam was focused on the sample with a 100x microscope objective (NA = 0. 85), with a laser power at the sample of < 2 mW.

TEM

The JEOL JSM-7401 F Field Emision transmission electron microscope with ultra high vacuum and 1 nm resolution was used to characterize both morphologies and elemental anlayse of the samples. Sample preparation was performed by dispersing 0. 1 g of sample in 50 ml of distilled water. The diluted dispersion was sonicated for 5 min to break apart sample agglomerations; afterwards, a drop of the dispersion was placed on a holey-carbon-cooper-grid. .

TGA

TGA analysis was achieved using a TA Instruments TQ-50. Samples for analysis were prepared taking required amount to evoporate in the oven. Then, approximately 10 mg of sample were weighed and put into aluminium cups. The characterization was performed using nitrogen atmosphere at heating rate 10 °C min^{-1} from ambient temperature to 900 ^{o}C**.**

CYCLIC VOLTAMMETRY

The electrochemical measurements were conducted using screen printed electrodes in a DropSense cyclic voltammeter potentiostat. For sample preparation, 0. 01 g of samples was dispersed in 5 m L of N-Methyl-2-pyrrolidone (NMP). Then, 2µL of each solution were drop casted onto to the carbon working electrode and dry under vacuum.

The electrolyte employed were HCl and buffered solutions of pH 2, 3, 5, 6. In the buffered solutions, 1 M of NaCl was added to maintain the ionic strength constant.

CONDUCTIVITY MEASUREMENT BY FOUR-PROBE TECHNIQUE

DC-Conductivity measurements were carried out using the four-probe method on rigorously dried pellets. The measurements were carried out using a four-probe setup equipped with a dc current source (LCS-02, Scientific Equipment & Services) and a digital micro-voltmeter (DMV-001, Scientific Equipment & Services). Prior to conductivity measurements, the polymers were redoped by 100 mL of 0. 1 M HCl under magnetic stirring. Before being filtered, washed with distilled water and dried under vacuum. Two types of PANI/SGrf (PANI/GSA and PANI/GNSA) and PAni/RGO composites of different mass ratio stored until needed for characterizations.

Electrical conductivity of the pressed pellets were calculated by potential-current data taken by four probe method using the Eq. 1 (Smiths, 1958).

$$\rho = \left(\frac{\Pi}{\ln(2)}\right) t \left(\frac{V}{I}\right) = 4.5324 t \left(\frac{V}{I}\right) \qquad (1)$$

Where *V* is the potential, *I* is the current, and *t* is the thickness of the pellets.

To calculate the resistivity of a sample of finite width and non-negible thickness; the equation (1) should be multiplicated with the correction factors f_1 and f_2 (Eq. 2):

$$\rho = \left(\frac{\Pi}{\ln(2)}\right) t \left(\frac{V}{I}\right) f_1 f_2 = 4.5324 t \left(\frac{V}{I}\right) f_1 f_2 \qquad (2)$$

Where ;

$f_1 = f_{11}\left(t/s\right)$ is the finite thickness correction for the insulating bottom-boundary pellets, where *s* is the probe spacing and;

$f_2 = f_{2c}\left(\frac{d}{s}\right)$ is the finite width correction, where *d* is the diameter of the pellets (Figure 13). f_{11} and f_{2c} values were obtained as described from graphics given by Smiths (1958)

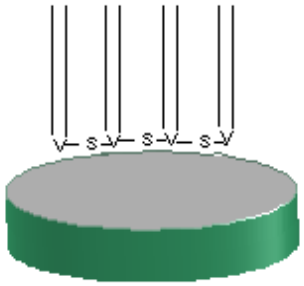

Figure 13: Four probe method

CHAPTER III

IX. RESULTS AND DISCUSSION

In the presented work two different experimental systems were studied.

PART 1

In the first part it is depicted the experimental observations of the aformentioned mechanism as it is proposed: The donor-aceptor interection between RGO sheets and PAni, while PAni in its leucoemeraldine state and graphene is oxided.

POLYANILINE / RGO COMPOSITES

Leucoemeraldine state of PAni obtained after polymerization of aniline can be oxidized to emeraldine state easily due to its instability. In the presence of GO, with expected electron transfer polyaniline is oxidized, and GO may be reduced. , as seen in the Figure. 14.

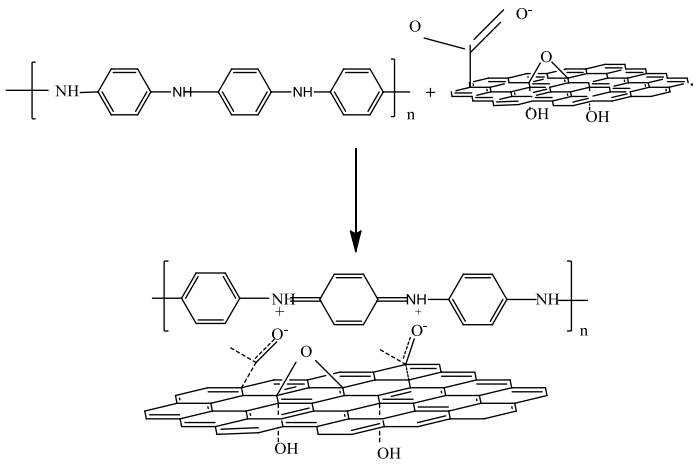

Figure 14: Proposed equation of oxidation of leucoemeraldine state of PAni by reduction of GO

POLYANILINE/GO COMPOSITES

In the same way, negatively charged GO sheets can perform as the doping agent of polyaniline, as seen in the Figure. 15:

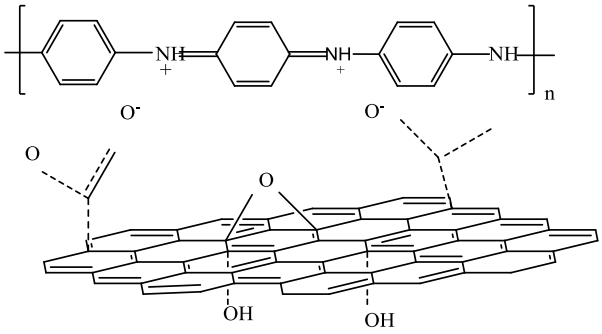

Figure 15. GO dopped polyaniline (PANI/GO)

1. UV-VIS and FT-IR spectra

The spectra of the samples in *N*-methyl-2-pyrrolidine (NMP) solutions are showed in Figure. 16. The concentration of the samples was 0. 1 mg mL^{-1} in all cases. The spectrum of PAni shows two bands. The band at 320 nm is assigned to the π to π * transition in the aniline ring. The band at 600–650 nm is assigned to the “exciton” transition of the quinonimine, and is related to the intra-chain hopping (Ginder *et al.* , 1990). The spectra of the Leucoemeraldine / RGO resembles that of PAni. The first signal appears at a smaller wavelength than PAni. It may due to steric effects between graphitic domains, which are less conjugated. The second band appears at longer wavelength than in the pure PAni. This little shift can be explained by the deprotonation of leucoemeraldine by dissociation of the carboxylate anions on the surface of the GO (Barbero *et al.* , 2004). In completely reduced leucoemeraldine, this polaron bands would not be displayed, but a unique absorption band around 340 nm (Valles *et al.* , 2011).

The spectrum of the GO shows the typical unique absoption band at 230 nm. This band shifted to longer wavelengths in leucoemeraldine / RGO, indicating that the electronic conjugation within the reduced graphene sheets was revived upon reduction of graphene oxide (Li *et al.* , 2008). Uv-spectrum points the leucoemeraldine state of polyaniline oxide, and the interaction between polyaniline and GO .

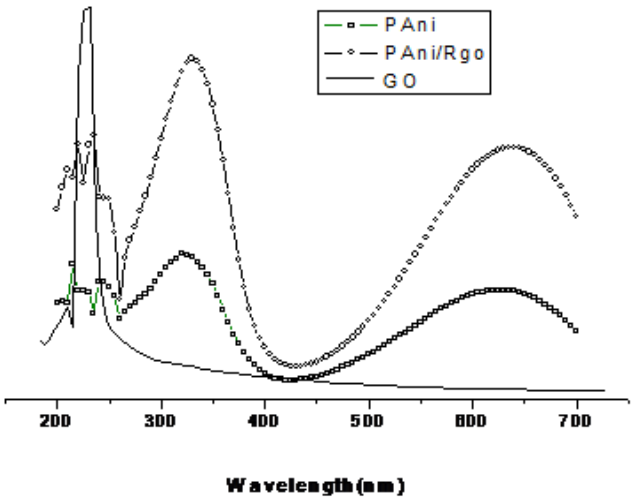

Figure 16. UV-VIS spectra of the PAni, PAni / RGO, and GO samples

FT-IR spectra of PAni, GO, PAni / RGO and PAni / GO were recorded in the region of 4000-450 cm^{-1} at ambient temperature, Figure. 17.

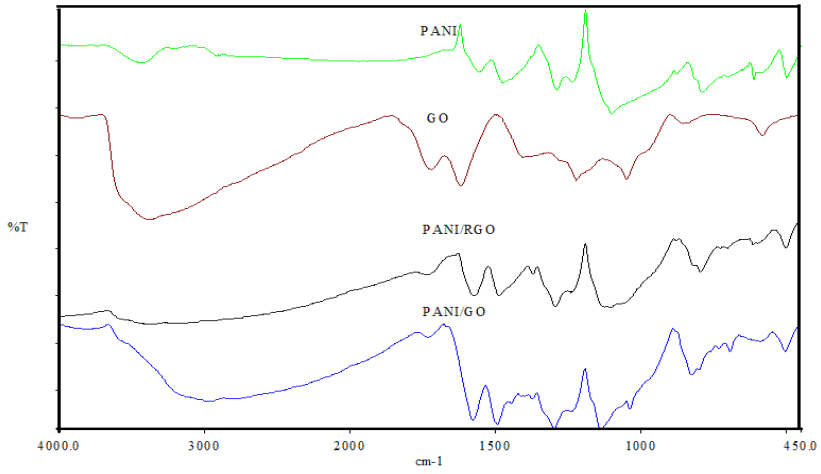

Figure 17. FT-IR spectra of pure PANI, GO, PANI/RGO and PANI/GO

According to the theoretical results of peak positions, the broad peak at the frequency of 3500 cm^{-1} and the weaker peak at the frequency of 2900 cm^{-1} indicate the N–H modes of N–H stretching in PAni spectra (Coskun *et al.* , 2012). For the pristine PAni, the absorption peaks located at 1600 and 1500 cm^{-1} are respectively ascribed as C=C stretching deformation of quinoid and benzenoid units of emeraldine salt. The peaks at the frequency of 1305 and 1260 cm^{-1} correspond to the C=N and C–N–C stretching modes in the benzenoid and quinoid imine units, respectively (Quillard *et al.* , 1994). When PAni was converted to PAni / GO, the peaks at 1600 and 1500 cm^{-1} became sharper. And the peak at 1260 cm^{-1} became weaker. This can be attributed to the π–π interaction between the two components, as well as hydrogen bonding.

The intensive peak at around 1150 cm^{-1} is attributed to C–N stretching for the benzonoid ring. (He, 2005). The peaks at 750, 600, and 500 cm^{-1} are assigned to C–H stretching mode. For GO, the characteristic vibrations include the broad and intense peak at 3450 cm^{-1}, which was attributed to O–H groups, highly saturated C=O peak in carboxylic acid and carbonyl moieties at 1700 cm^{-1}. The peaks at 1400 and 1250 cm^{-1} were attributed respectively to C–OH and C–O–C groups. The sharp peak at 1070 cm^{-1} and the weaker peak at 850 cm^{-1} was assigned to C–O stretching in C–OH functional groups and aromatic C–H peak, respectively (Wang *et al.* , 2009). The peak centered at 1590 cm^{-1} was assigned to adsorbed water, but it may be also related to the presence of components from skeletal vibrations of unoxidized graphitic domains (Yan *et al.* , 2010).

In the PAni / RGO composite, considering basic repeating monomer unit of PAni, new peaks were attributed to RGO. Comparing to PAni / GO composite in the spectrum of PAni / RGO the intensity of the O–H peak at the frequency of 3200 cm^{-1} and the intensity of the C=O peak at 1700 cm^{-1} become weaker. It is the evidence of the removal of the oxygen functional groups. In the spectrum the peaks between 1100 and 1650 cm^{-1} are associated to the stretching vibrations of both double and single C–N and C–C bonds, and the stretching of C–H bonds of the PAni.

By comparison, the spectra of the PAni / GO and PAni / RGO composites illustrate the obvious presence of PAni characteristic vibrations, suggesting PAni can be successfully presented on the GO and RGO surfaces.

2. Cyclic voltammetry

The characterization processes of cyclic voltammetry (CV) involve redox reactions, which are based on the transfer of electrons from a reductant to an oxidant. To further confirm the electrochemical activity of the PAni composites and asses the protonation-oxidation states of the PAni, the electrochemical properties of the composites were characterized by this technique. CV was run on the PAni and PAni / RGO in electrodes.

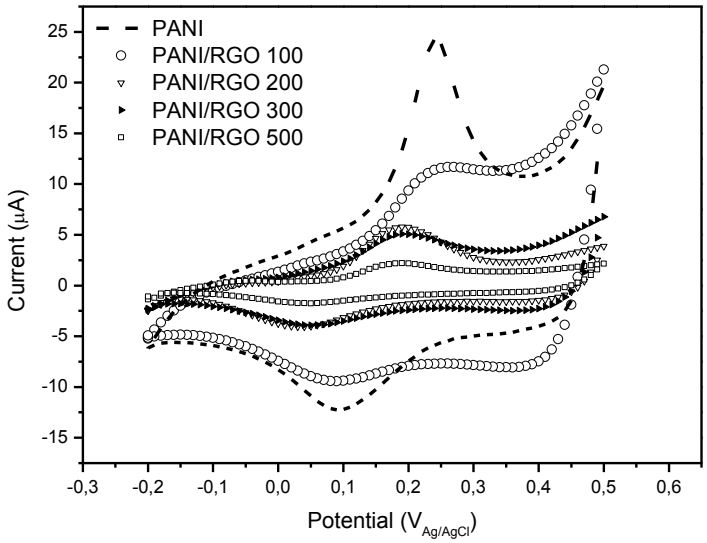

Figure 18. Voltammograms at 100 mV s^{-1}

Both PAni and other electrode materials show a redox pair, which mainly results from transition of the PAni leucoemeraldine form to its conducting state, which is the emeraldine form as seen in Figure 18. The peaks show that PAni / RGO composites are electrochemically active. The peak positions of the graphene based materials are down shifted. It can be ascribed as the effect of the changing in PAni structure doped by graphene based materials. The electrochemical performances have been affected by the mass ratio PAni : RGO. According to the Figure, PAni / RGO 100 exhibits closer electrochemical performance to PAni.

In Figure 15, the electrochemical performance of the PAni / RGO 100 electrode material was analyzed at 20, 30, 50, 100, or 200 MV s^{-1} scan rates.

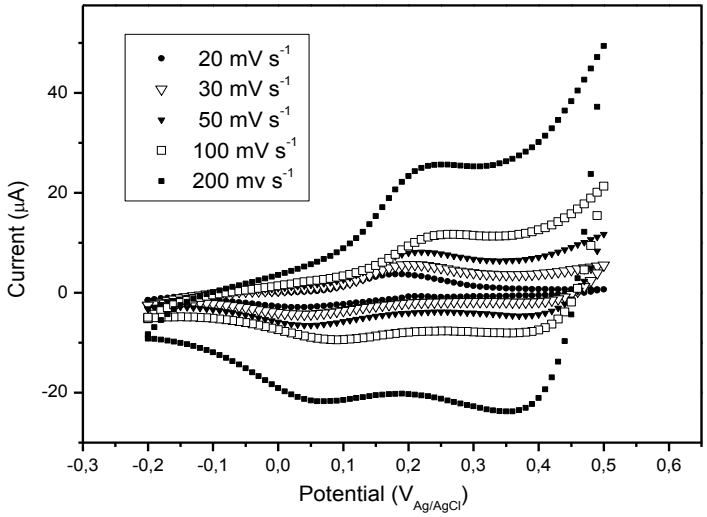

Figure 19. Cyclic voltammograms of the PAni / RGO 100 composite at different scan rates

The specific capacitance of the electrodes was calculated according to Eq 3: (Wang *et al. ,* 2010):

$$C=(\int I \, dV) / (v \, m \, V) \qquad (3)$$

Where the *C* is capacitance (F g^{-1}), *I* is the current density (A g^{-1}), *v* is the potential scan rate (mV s^{-1}), *m* is the mass of the electroactive materials in the electrodes and *V* is the potential. As shown in Figure 18, the area of the positive part of the CV curves was used for specific capacity calculation. According to this equation, the calculated specific capacitances of the PAni / RGO materials was 20 mV s^{-1}. The scan rates are listed in the Table 1. These values are lower than pure PAni specific capacitance (117. 7 F g^{-1}) and those given by Wang *et al.* (2010) due to the different route of synthesis.

Table 1. Specific capacities of the materials

Material	Specific Capacitance (F g^{-1})
PAni / Rgo 100	90. 97
PAni / Rgo 200	31. 41
PAni / Rgo 300	36. 72
PAni / Rgo 500	13. 82

The calculated specific capacities of the PAni / GO material was 170 F g^{-1}. For the electrical conductivity studies, powders of each material have been pressed to obtain pellets. The electrical conductivities of the materials were determined on pressed pellets by the four probe technique. The potentials for each current were collected and the average resistances were calculated. After resistance, resistivity, and conductivity were calculated. The electrical conductivities of the PAni, PAni / GO, PAni / RGO 100, PAni / RGO 200, PAni / RGO 300, and PAni / RGO 500 were 0. 845, 0. 44, 0. 279, 0. 06, 0. 05, 0. 02 S cm^{-1}, respectively. The electrical conductivity is the best indicator that GO was reduced to graphene. So it is possible to say, in the case of PAni / RGO composites that the GO was successfully reduced.

PART 2

In the second part, it is depicted the experimental observations of the aformentioned mechanism as it is proposed: Modification of the graphene by sulfonation and its functionalization to PAni.

Modification of reduced graphene

The synthesis of the two different reduced graphene was as follows: Sulphanilic acid was first converted to diazonium salt by sodium nitrate in acidic media. Then, it was converted to a radical by temperature effect as seen in Figure 20 (Lomeda *et al.* , 2008). The graphene was sulfonated by coupling with the diazonium salts.

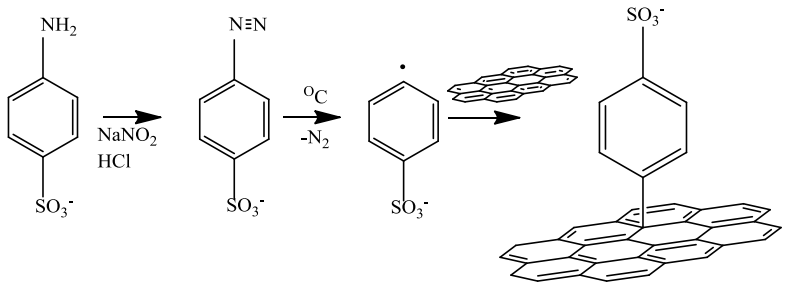

Figure 20. Sulphanilic acid and reduced graphene sheets

The same process was performed for 6-amino-4-hydroxy-2-naphthalenesulfonic acid as seen in Figure. 21 (Lomeda *et al.* , 2008)

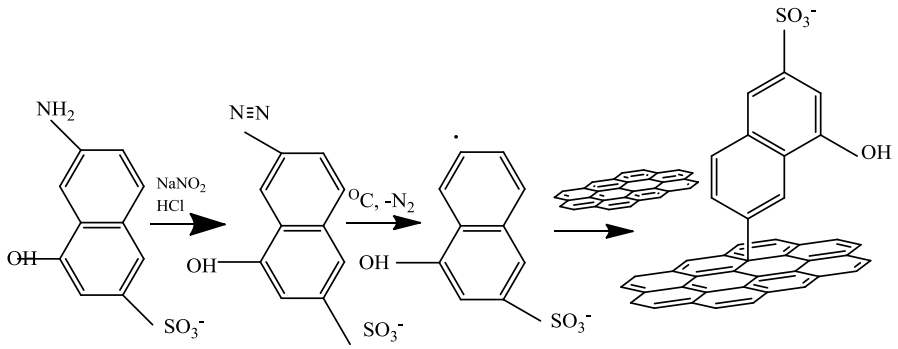

Figure 21. 6-amino-4-hydroxy-2-naphthalenesulfonic acid and graphene sheets.

***In situ* polymerization of polyaniline**

The composites were prepared by polymerization of aniline in a solution containing dispersed sulfonated graphene by in situ polymerization method. Under this condition, the negatively charged graphene sheets have sufficient electrostatic repulsion to affect the polyaniline as seen in Figures. 22 and 23 (Si and Samulski, 2008):

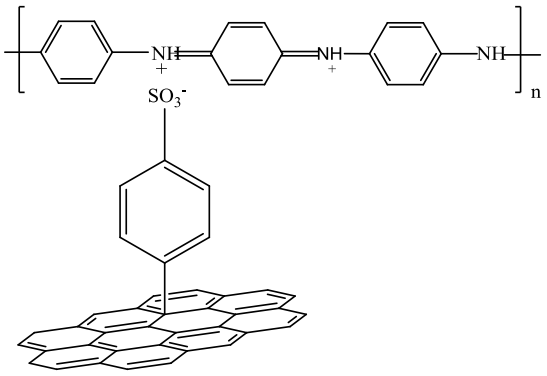

Figure 22 : RGO-SA dopped polyaniline (PANI/GSA)

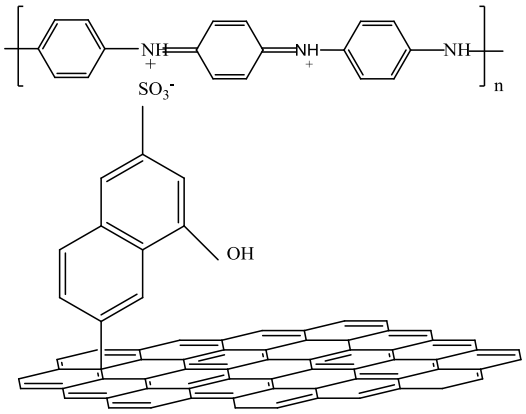

Figure 23. RGO-NSA dopped polyaniline (PANI/GNSA)

1. UV-VIS and FT-IR spectra

The UV–visible spectra of PAni / GSA and PAni / GSA resemble that of PAni as shown in Figure. 24.

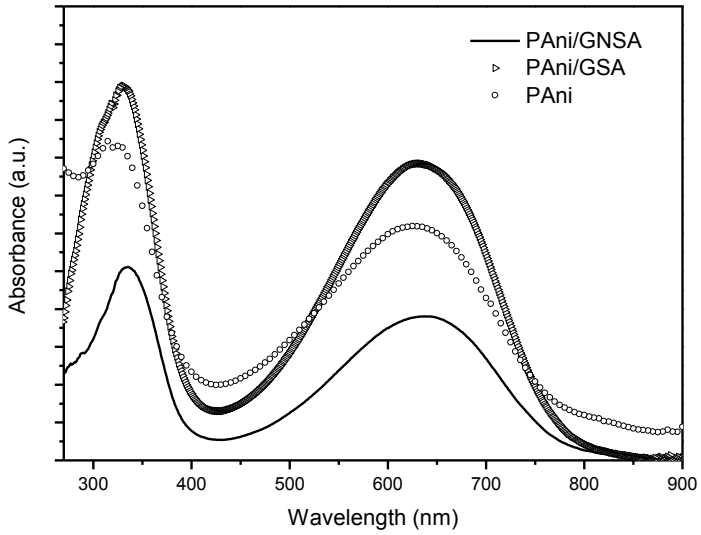

Figure 24. UV-VIS spectra of the PAni, PAni / GSA, and PAni / GNSA

The spectra of pure PAni in NMP show two bands at 330–334 nm (attributed to π–π^* transition) and 632–635 nm, which were assigned to the transition of the exciton of the

quinone and related to the hopping electronic intra- and inter-chain. In the spectra of the PAni / GSA and PAni / GNSA, the first signal appears at a longer wavelength than in PAni. It may probably be due to a steric effect caused by the huge graphitic laminates that makes the transition energy to increase. Furthermore, it is also noted that the polaronic band shifts to lower energy in the case of both sulfonated materials. It has been reported that the λ_{max} of this band depends on the polymer oxidation, so the shift can be produced by some doping of PAni with GSA and GNSA (Straftrom *et al.* , 1987; Master *et al.* ,1991).

Chain conformation plays a critical role in the properties of polyaniline. The study of the electronic structure of the protonated polyaniline is complicated by the simultaneous presence of different structures (Ivan *et al.* , 2004). This further conformed by UV-vis spectrometry. To investigate this dependence in the PAni composites, the composites were doped by HCl. The solutions of the protonated states of the composites showed yellow color. The doping does not practically affect the shape and the place of the band in the wavelength range of 340 nm. The spectra show a new polaronic band at 420 nm, as seen in Figure. 25. And the initial polaronic band moves to larger wavelengths (800–900 nm) due to the external protonation. This absorption peak originates from the polaron band transition. In addition, the position of the peak at 340 nm does not change with its protonation state although the intensity of the band decreases. This indicates that the proton process only takes place on the imine segment on the emeraldine chain (Fu and Weiss, 1997)

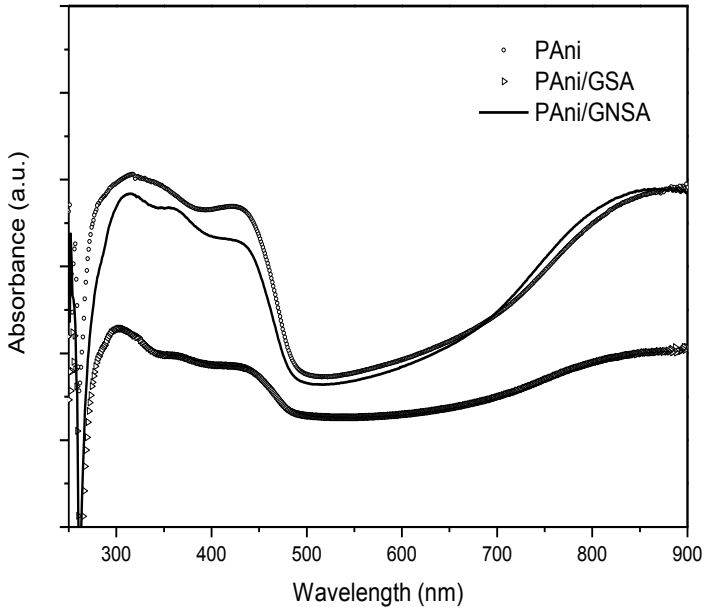

Figure 25. UV-VIS spectra of the doped PAni, PAni / GSA, and PAni / GNSA

In order to check whether or not the different sulfonation degree translates in different solubility; we carried out UV–visible experiments in water for the sulfonated graphenes as seen in Figure 26. The peak at 248 nm can be commented as the typical peak of graphene. Oppositely in this spectrum, GSA has showed the sulfonate peak around 550 nm.

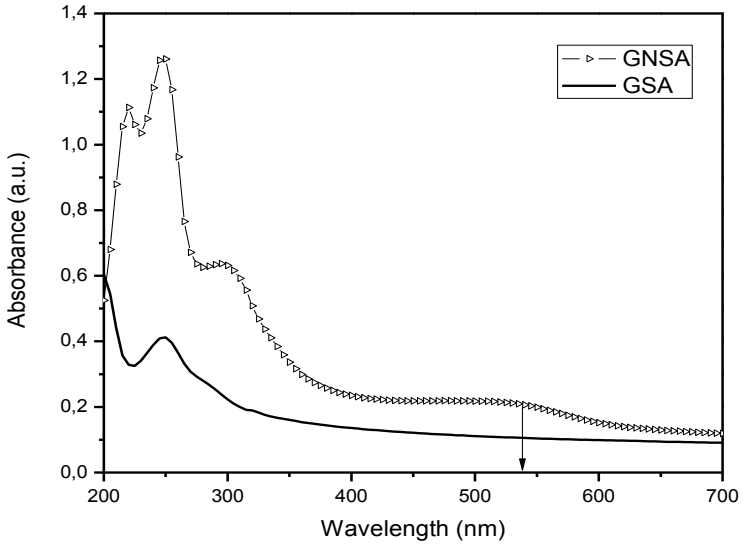

Figure 26. UV-VIS spectrum of the GSA and GNSA in water

Sulfonated graphene by coupling with the diazonium salts of sulphanilic acid and nafthalene sulfonic acid give products that are soluble in water (Si and Simulski 2008). The solubility was calculated, using the experimental absorption coefficient for graphene dispersion in surfactant solutions (1390 L g^{-1} m^{-1}) (Lotya *et al.* , 2009). The absorption coefficient α, which is related to the absorbance, *A*, through the Lambert-Beer law (*A*) α *C* ***l***, where *C* is the concentration and ***l*** is the path length, is an important parameter in characterizing any dispersion (Lotya *et al.* , 2009). Calculated water solubility of the sulfonated graphene materials are given below. Although this procedure is somewhat different from other approaches involving a pre-reduction step it is also successful.

$$\alpha = 1390\, mL/mg * m$$
$$[C] = A/(0.01m)(1390 mL mg^{-1} m^{-1})$$
$$[C]_{RGO-SA} = 0.09/13.9 mL mg^{-1}$$
$$[C]_{RGO-SA} = 6.47 * 10^{-3}\, mg/mL$$
$$[C]_{RGO-SA} = (6.47 * 10^{-3}\, mg/mL) * 16 = 0.104\, mg/mL$$
$$[C]_{RGO-NSA} = 0.012/13.9 mL mg^{-1}$$
$$[C]_{RGO-NSA} = 8.63 * 10^{-3}\, mg/mL$$
$$[C]_{RGO-NSA} = (8.63 * 10^{-3}\, mg/mL) * 16 = 0.138\, mg/mL$$

The FT-IR spectra were run for the composites of both sulfonated materials as seen in the Figure 27. The spectra of PAni / GSA and PAni / GNSA composites presented the typical bands of PAni at 1560 cm^{-1} (C=N, quinoid ring (Q) stretching), 1480 cm^{-1} (C–C benzenoid ring (B) stretching), 1292 cm^{-1} (C–N stretching of secondary amine), 1235 cm^{-1} (C–N in BBB units), 1115 cm^{-1} (C–H in plane bending of aromatic rings), 817 cm^{-1} (C–H deformation in Q ring), and 796 cm^{-1} (C–H out of plane bending of aromatic rings). It is remarkable the presence of two new bands in the sulfonated compounds, located at 1372 cm^{-1} and 1260 cm^{-1} (Trchova and Stejskal, 2011). While the first has already been observed in PAni and is assigned to C–N stretching in QBQ units; whilk the second has been observed in doped PAni (Boyer *et al.* , 2000), suggesting that some internal doping of PAni by SG takes places. This is in agreement with a previous study on the doping of PAni with reduced graphene oxide, where the formation of a solid state charge transfer complex has been proposed. Finally, a shoulder can also be observed at 1034 cm^{-1}, which was attributable to the symmetric SO_3 stretching in the SG counterion.

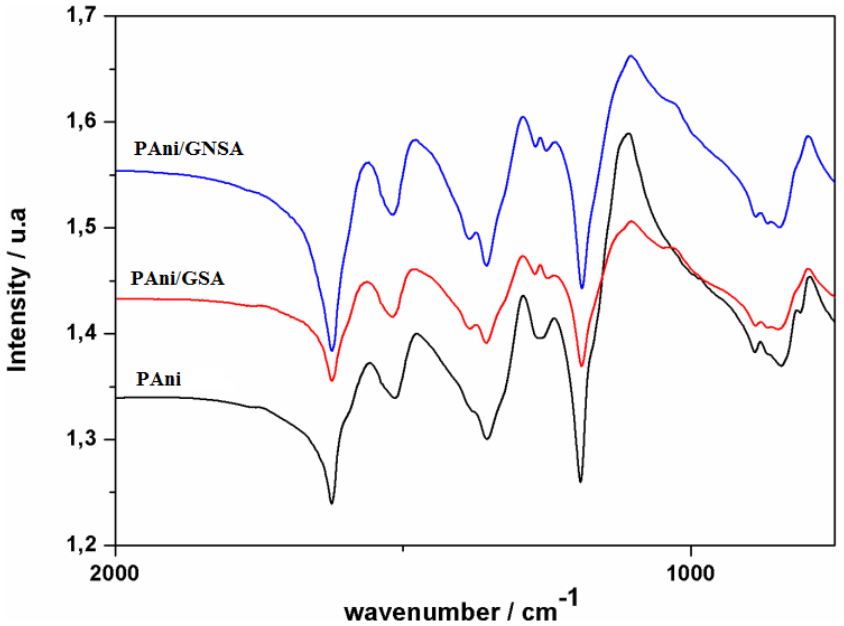

Figure 27. FT-IR spectra of the PAni-sulfonated graphene composites

The FT-IR spectra of both sulfonated graphenes were also run (Figure. 28). In sulfonated compounds the spectra display clear bands at 1095 and 1037 cm^{-1}, which are assigned respectively to the symmetric and anti-symmetric stretching of sulfonic groups (Salavagione *et al.* , 1999). The absence of the second peak in the RGO-NSA spectrum can be due to overlapping. The other peaks in the spectra were attributed to typical peaks of carboneous materials. C=C stretching of aromatic ring (1554 cm^{-1}), C–H stretching (1384 cm^{-1}), C–H in plane bending of aromatics (1162 cm^{-1}), and C–H out of plane bending (803 cm^{-1}).

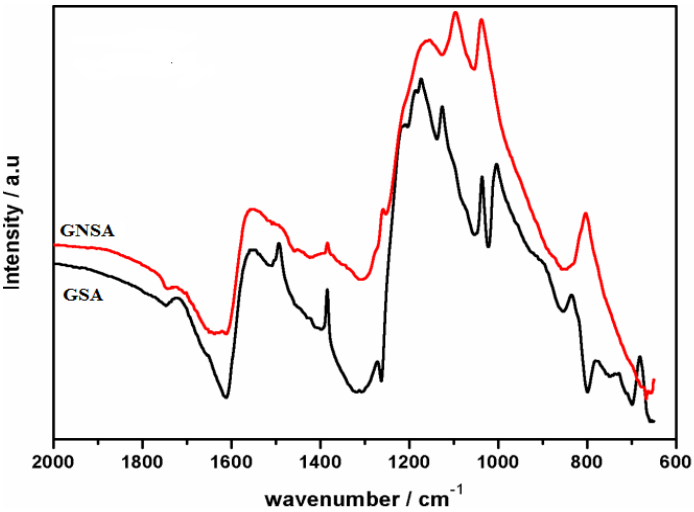

Figure 28. FT-IR spectra of the GSA and GNSA materials

2. Tga

TGA was used to determine the degree of sulfonation by comparing the weight loss of the SGrfs and GO starting material. Figure. 29 shows the traces of GO, RGO-SA and RGO-NSA. In the case of GO, the mass loss started below 200^{0}C, and was fast at nearly 210^{0}C %.

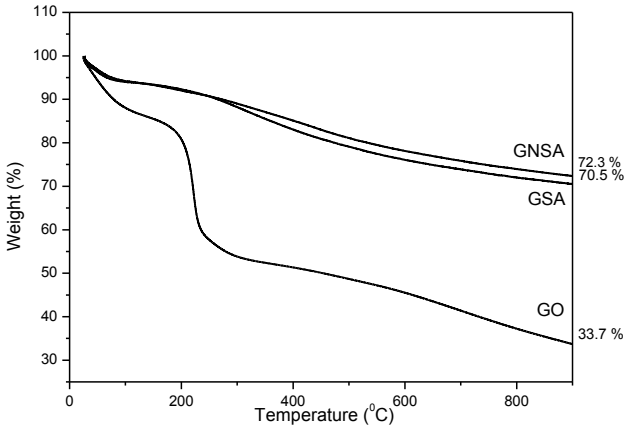

Figure 29. TGA curves of GO, GSA and GNSA

At the end of the analysis, the weight loss of the GO was nearly 66%, this behavior was attributed to pyrolysis of the oxygen containing groups such as –OH, –COOH, *etc*. The weight losses of the SGrfs were between 27 and 30%. SGrf materials were found to suffer of less weight loss due to functionalization between the reduced graphene and sulfonation groups. This indicated that less volatile functionalities are present on RGO-SA and RGO-NSA surfaces comparing to GO as a result of the successful reduction. Consequently, the two sulfonation methods described here gave thermostable compositions. In addition, according to the weight loss, the methods gave nearly the same sulfonation degree.

3. Raman Spectroscopy

Raman spectroscopy is a powerful tool to determine the microstructure of the carbon-based materials. Therefore, Raman measurements were conducted in order to characterize the sulfonated graphene, as seen in Figure 30. Raman spectrum of the GO shows the D and G bands respectively at 1352 cm^{-1} and 1598 cm^{-1}. The D band corresponds to defects in the sp^2 lattice, while the G band is related to the sp^2 carbon network. For modified-RGO materials, the spectra also show the prominent peaks at 1353 cm^{-1} for GSA and GNSA, which are assigned to the D band. The high intensity of the D band in both cases is because of the starting material is GO, which is highly defective. The materials showed the G bands shifted to around 1589 cm^{-1} (GSA) and 1575 cm^{-1} (GNSA) towards the value for graphite. This was related to the high number of defects (Coskun *et al.* , 2012).

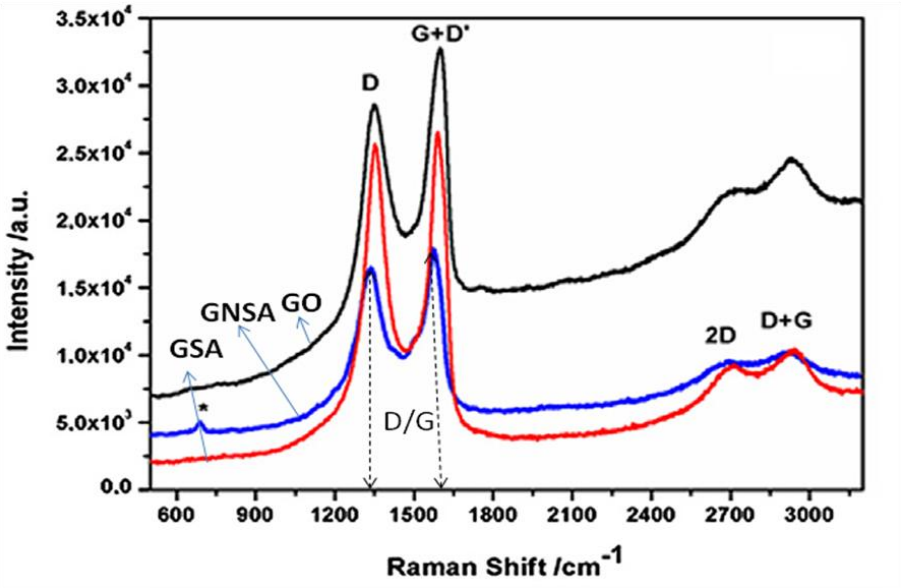

Figure 30. Raman spectra of the GO, GSA, and GNSA

The D / G intensities of the samples were calculated. The values for GSA, GNSA, and GO were respectively of 0. 96, 0. 92, and 0. 87. The D peaks intensities got higher in both sulfonated graphenes because of the formation of smaller graphitic domains than those in GO. (Stankovic *et al.* , 2007). In Figure. 26, the 2D peaks at 2700 cm^{-1} are also detected. This peak sometimes referred to as G′, which is a second order vibration caused by the scattering of phonons at the boundary zone (Ferrari *et al.* , 2006). Surprisingly, despite the high Raman efficiency of the D and G signal, another weak peak is perceived at 710 cm^{-1}. This peak can be assigned to C–S aymmetric stretching, suggesting a reasonable degree of modification, contrary to the FTIR results (Coskun et al, 2012)

4. Cyclic Voltammetry Studies

To further confirm the electrochemical activity of the PAni composites, and asses the protonation-oxidation states of the PAni, the electrochemical properties of the composites were characterized by cyclic voltammetry (CV). Thin films of both composites were prepared on the working electrode of screen-printed electrodes. The CV was run on the PAni / GSA and PAni / GNSA lectrodes in 1M HCl solution electrolytes with a potential from -0. 2 to 0. 8 V, as seen in the in different scan rates in Figure 30.

Literature shows voltammograms with two-well defined and a one middle reversible protonation and oxidation peaks of redox processes characteristic of PAni. These are assigned to oxidation and protonation of the polymer chain (Macdiarmid *et al. ,* 1987). The cyclic voltammograms of both PAni / GSA and PAni / GNSA in 1 M HCl electrolyte show a similar behavior to that of pure polyaniline. Similarly to PAni, the first peak is attributed to leucoemeraldine / emaraldine transition of PAni; whereas the second peak, is assigned to emeraldine / perningraniline transition in the PAni. When the sweep starting from –0. 2 V, there was no appreciable current flowing through the electrodes up to about 0. 2 V. So between -0. 2 to 0. 2 V the polymer was completely at its reduced state, which corresponds to the leucoemeraldine form. As the potential increases, the first peak appears at 0. 25 V. This is the conversion of the leucoemeraldine form to the emeraldine form of PAni. The materials keep themselves in partially oxidized state until another transition (Figure. 31). The second peak between between 0. 6–0. 8 V is assigned to conversion of PAni from emeraldine to perningraniline state.

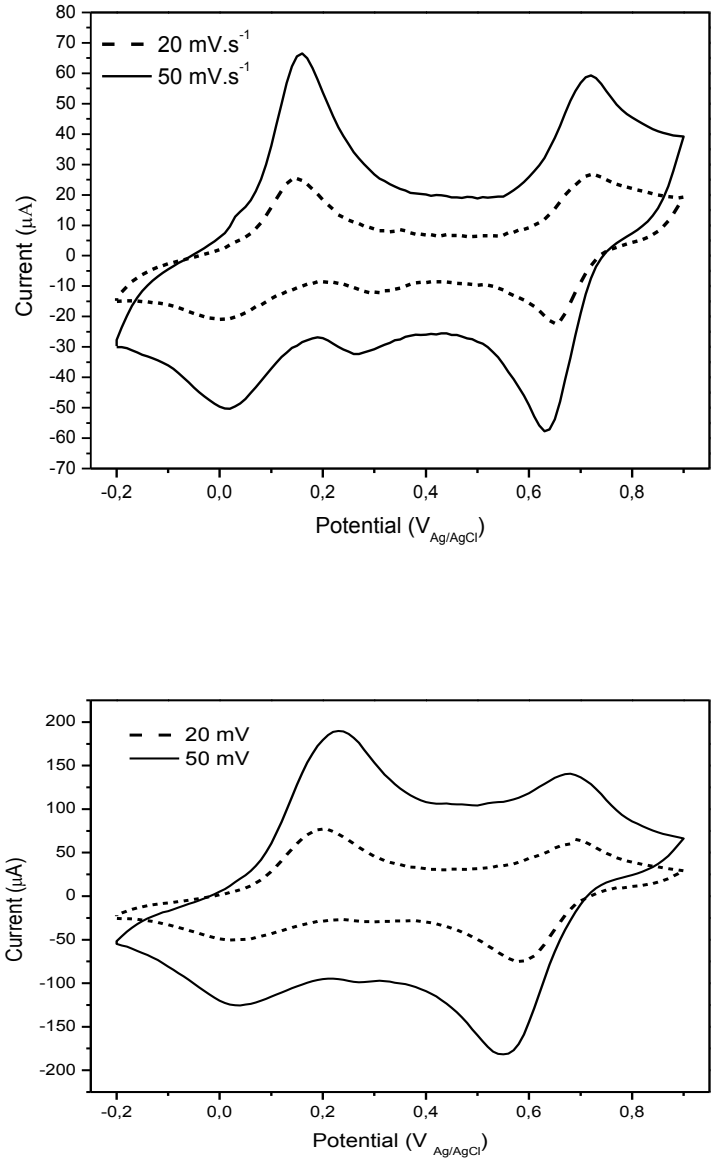

Figure 30. Cyclic voltammograms of a) PAni / GSA, and b) PAni / GNSA composites at different scan rates.

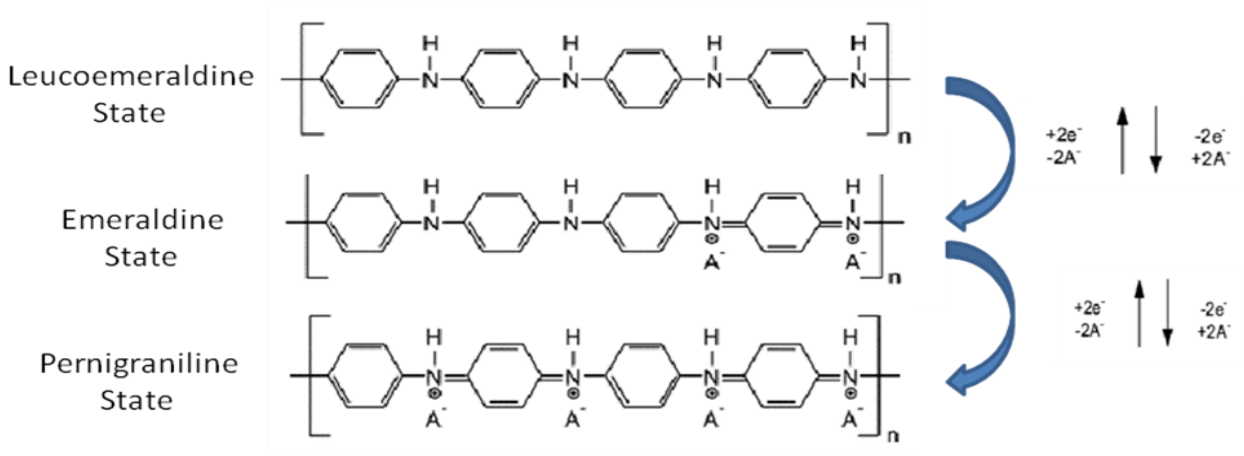

Figure 31. Conversion from emeraldine salt to pernigraniline

The CV of PAni, and PAni-sulfonated graphenes was run until 0. 6 V for the comparison of first oxidation peak, as seen in Figure. 32. The oxidation peak, corresponding to the transition between the leucoemeraldine and emeraldine state of the polymer, slightly shifted to higher potentials in the sulfonated materials with respect to the pristine PAni. Probably, the sulfonic groups in graphene withdraw electrons from the aromatic ring, making the amine units more difficult to oxidize. In other words, this effect can also be related to the doping of PAni with the sulfonated graphene.

In order to check the electroactivity of PAni / GSA, and PAni / GNSA materials in different environments, including physiological pHs, we conducted cyclic voltammetry in electrolytes with different pHs (Figure 33). Electrolytes of 1 M HCl (pH 0) and pH 2 solutions from HCl, electrolytes of pH 3 and pH 5 solutions from acetic acid, electrolytes of pH 6 from phosphate were prepared.

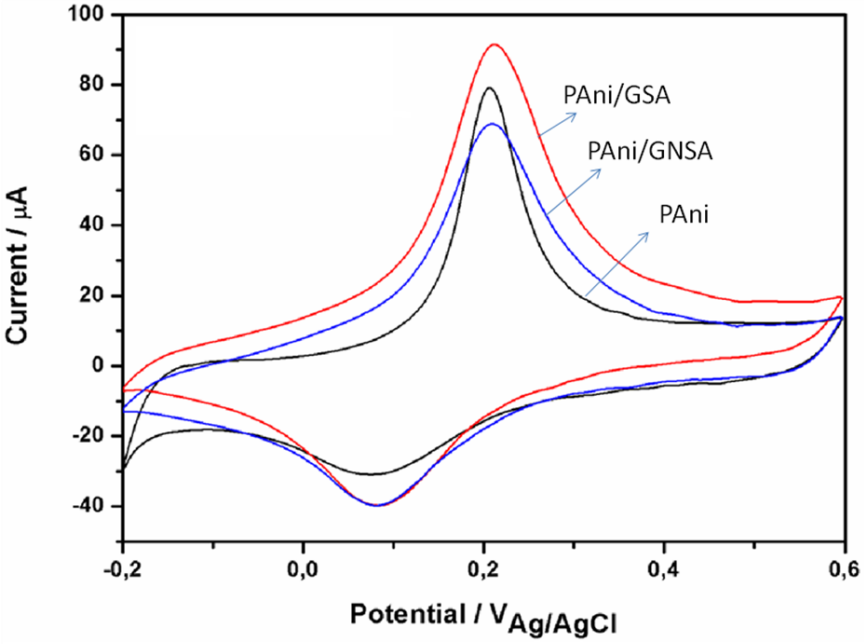

Figure 32. CV voltammograms of the composites until 0. 6 V

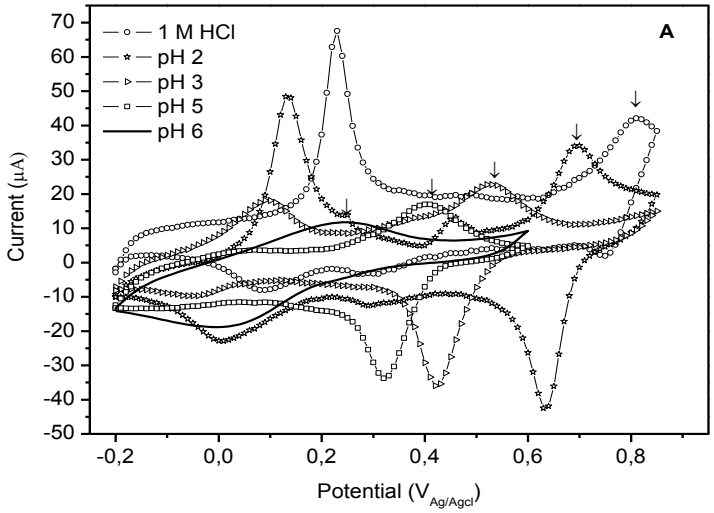

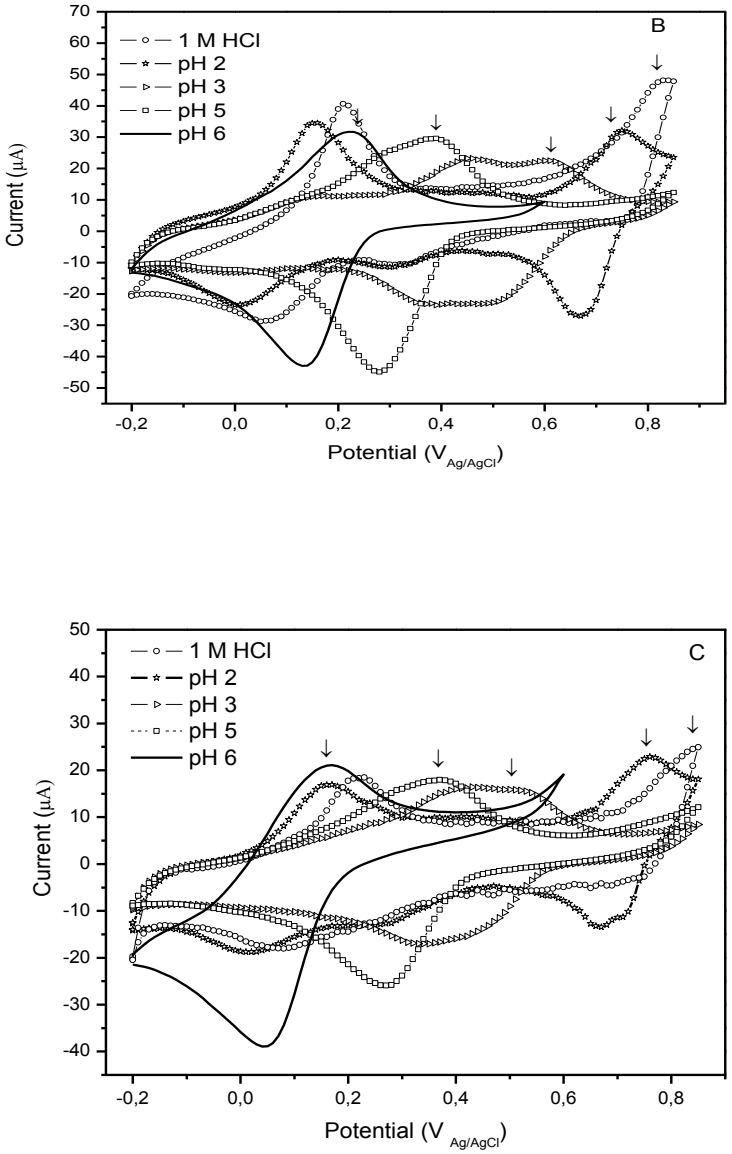

Figure 33. Cyclic voltammograms of a) pure PAni, b) PAni / GSA, and c) PAni / GNSA in different pHs at 20 mV. s^{-1}

As seen from Figure 33, both hybrids show improved electroactivity, remaining electroactive at higher pHs. Similarly to pure PAni / GSA and PAni / GNSA, the hybrids

showed both peaks, corresponding to the leucoemeraldine / emeraldine and emeraldine / pernigraniline transitions of PAni. While the pH increases second oxidation peaks of the materials shift to lower potentials, as seen in Figure 33. At the higher pHs, they even tend to overlap at an intermediate potential. This very interesting feature indicated that the transition leucoemeraldine / emeraldine became more difficult, while the transition emeraldine / pernigraniline became easier, as the pH increased. However, in the case of PAni / GSA and PAni / GNSA, after overlapping, the new peak moves to lower potentials as the pH increases, following the tendency of the second peak. In other words, the second transition varies similarly to PAni; but the first transition potential increases at lower pHs, and then decreases as the pH increases. In the case of PAni, this process is independent of the pH, and only anion insertion occurs (Si and Simulski, 2008; Zhao *et al.* , 2011). The reasons for this are uncertain, and could be related to i) a change in the ion exchange mechanism of the first process, i. e. the polymer releases protons during oxidation up to a certain value of pH, and over this pH it start to uptake protons or ii) the disappearance of one of the intermediate states of oxidation of PAni.

The dependence of the electrochemistry of PAni/GSA and PAni/GNSA on the pH can be described with relations of redox peak portantial. According to Table 2, potentials *versus* pH values of the composites are used for the ion exchange calculation.

Table 2. Potential values at 1st and 2nd oxidation conversions

SAMPLE		$Ep_{ox\ 1}$	$Ep_{ox\ 2}$	$Ep_{red\ 1}$	$Ep_{red\ 2}$
PAni / GSA	1M HCl	0. 21	0. 83	0. 74	0. 06
	pH 2	0. 16	0. 75	0. 67	0. 01
	pH 3	0. 15	0. 60	0. 44	0. 44
	pH 5		0. 39		0. 28
	pH 6		0. 22		0. 13
PAni / GNSA	1M HCl	0. 22	0. 84	0. 69	0. 08
	pH 2	0. 16	0. 76	0. 67	0. 03
	pH 3	0. 41	0. 52	0. 43	0. 34
	pH 5		0. 37		0. 27
	pH 6		0. 17		0. 05
PAni	1M HCl	0. 23	0. 81	0. 75	0. 09
	pH 2	0. 13	0. 71	0. 64	0. 01
	pH 3	0. 09	0. 53	0. 42	-0. 05
	pH 5		0. 41		0. 032
	pH 6		0. 24		0. 02

The experimental points for PAni/GSA and PAni/GNSA, obtained from Table 2 are used to plot the graphics of variation of potential with the pH Figure. 34. The data for PANI are also shown for comparison. As seen, the linear relation exists between the second oxidation potentials and pH.

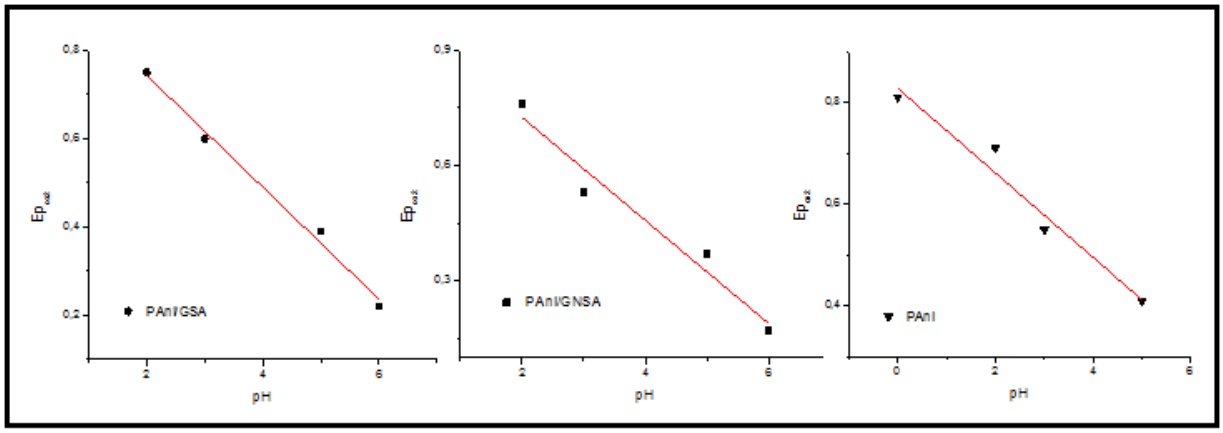

Figure 34. 2nd oxidation potentials *versus* pH values of the composites

The second oxidation values are used for the Nernst equation (Eq. 4), which allows to estimate the number of electrons and protons entering / leaving (the n_H / n_e ratio) the polymer composition, where E_p calculated from the slope of the E_p *versus* pH lines (Figure. 34) and E_f contains all terms not affected by the pH.

$$E_p = E_f - 0.059 \frac{n_H}{n_e} pH \qquad \text{Eq. 4}$$

The slopes of PAni / GSA (134mV) and PAni / GNSA (137mV) are similar to that of PAni (118 mV). This means that both composites expel 4 protons and uptakes 2 electrons (Salavagione *et al.* , 2003) as shown in the Table 3.

Table 3. Dependence of the peak potential on pH for second redox processes.

Material	**Slope (V / pH)**	**n_H / n_E**	**Ion exchange**
PAni / GSA	-0. 134	2	$4H^+ / 2e^-$
PAni / GNSA	-0. 137	2	$4H^+ / 2e^-$

Cyclic voltammetry was run at scan rates of 20, 30, 50, 70, or 100 mV s^{-1} for the PAni / SGrfs. It was found that maximum value of oxidation peak currents were proportional to the scan rates, and also to the square roots of scan rates (Figure. 35).

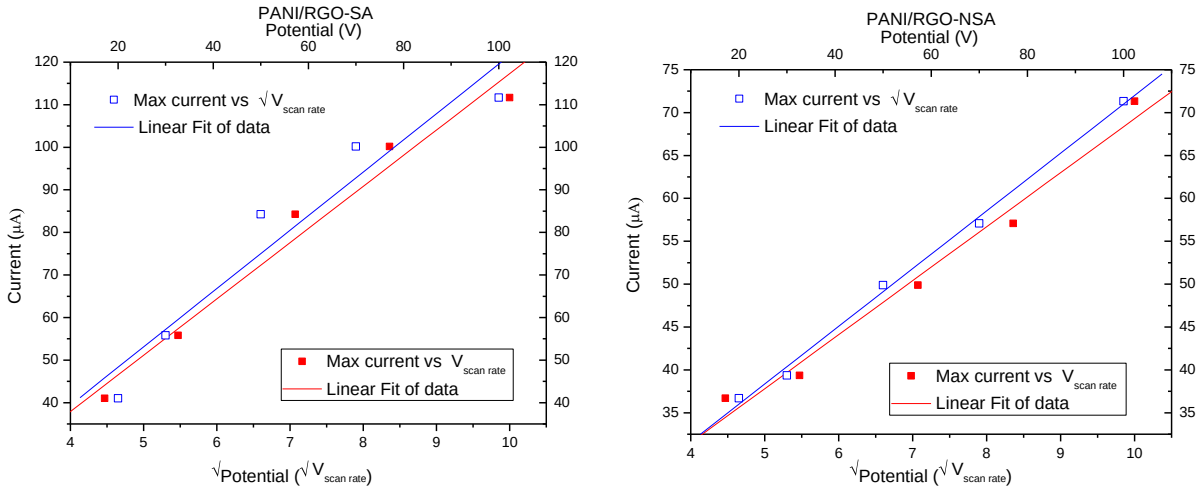

Figure 35. The relationship between the maximum oxidation peak currents and scan rate, the relationship between the maximum oxidation peak current, and the square roots of the scan rate in PAni / SGrfs

The same results have been reported by Chen *et al.* (2011), which is an indication of the incorporation of the SGrf onto the PAni. In fact, a good electrochemical response is obtained at pH 6. Differently to self-doped PAni, where the sulfonate groups take part of the polymer chain; here the sulfonated graphene sheets are trapped into the polymer.

The electrical conductivity of the products was calculated by potential-current data taken by the four probe method. As illustrated in Table 4, in our products, the pure PAni exhibited the lowest electrical conductivity compare to sulfonated products. Thanks to the higher conductivities of the SGrfs, conductivity has significantly increased in the polymer / graphene composites. It can be commented that the sulfonation of graphene creates favorable interaction and enhance the electron mobility between the PAni and the SGrf, which results in the elevated electrical conductivity compared with the pure PAni and SGrf alone. The GNSA products showed higher conductivity than the GSA products. It may commented as it is favorable to expand the graphene sheets more and/or provide better interconnection between graphene and polyaniline due to its moleculer structure.

Table 4. Electrical conductivity of the products

Material	**Conductivity (S cm^{-1})**
PAni	1. 42
GSA	13. 60
GNSA	14. 09
PAni / GSA	25. 60
PAni / GNSA	26. 33

4.1. Sensor Application

Taking profit of the electroactivity at higher pH, we carried out series of experiments to detect ferrocenium (Fc^+) at pH 6 (Figure 36).

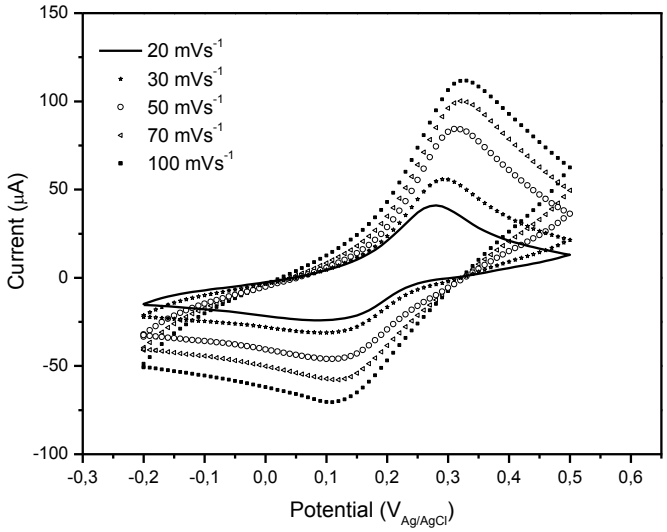

Figure 36. Cyclic voltammograms of PAni/GSA composite electrodes in phosphate buffers (pH = 6) + 1mM ferrocenium solution at different scan rates.

Cyclic voltammograms of the PAni / GSA composites in the electrolyte of pH 6 in the presence of 1 M Fe, show clear electroactivity, which is similar to the one in Figure. 32. While the scanning rates increased, the current of the first oxidation redox increase.

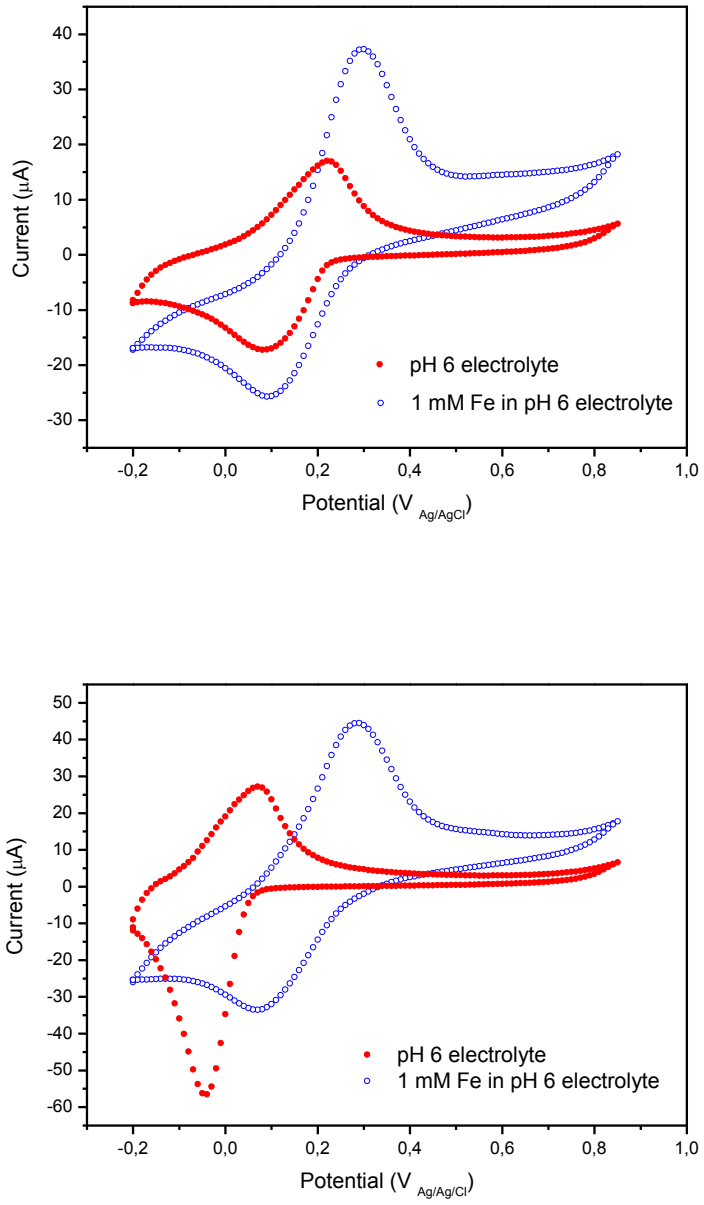

Figure 37. Cyclic voltammograms of PAni / GSA and PAni / GNSA materials in phosphate buffers (pH = 6) and 1 mM ferrocenium solution in phosphate buffers pH 6

PAni / GSA and PAni / GNSA gave clear oxidative responses both at pure pH 6 electrolyte and Fc in pH 6 electrolyte (Figure. 36). The detection of Fc was determined by the shifted peaks of composites in the electrolyte of Fc in pH 6 compare to pure pH 6 electrolyte. PAni / GSA composite´s oxidation peak was shifted to higher potentials, and observed between 0. 2–0. 4 V. PAni / GNSA composite´s oxidation peak is also shifted to higher potentials and observed at ca. 0. 3 V. The reductive responses were also observed between -0. 5–0. 1 V for PAni / GSA and -0. 05–0. 0 V for PAni / GNSA. These shifts, explained by the redox transitions of the composites, are strongly depends on the electrolyte. Also peaks are observed in the higher currents. This can be explained by the adsorption of the Fc on the electrode surface (Sanchis *et al.* , 2008).

5. Morphology Studies

The morphology and structure of the SGrf (GSA) composite are shown in Figure 38.

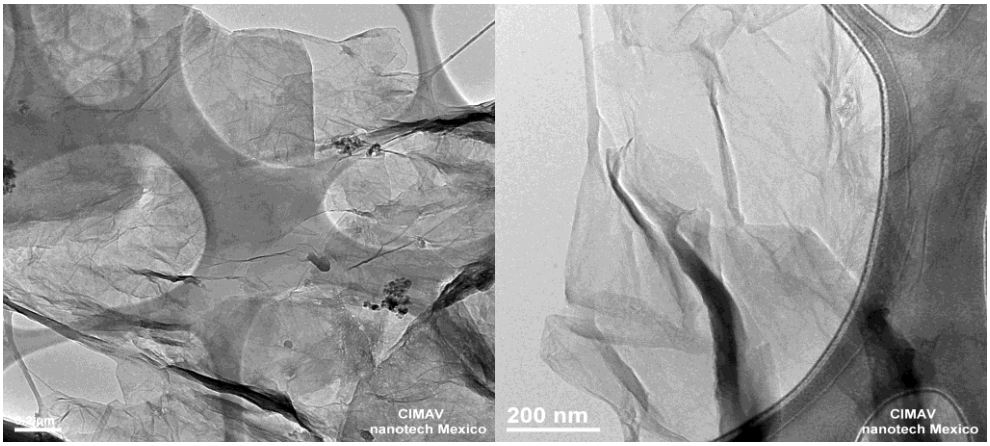

Figure 38. High resolution micrographs of GSA at different magnitude.

The wrinkled morphology of the GNSA composites, particularly on the edges of the samples, are different from the graphene sheets (Figure. 39) reduced by potassium borohydride ($KBrH_4$), suggests that that the type of reducing agent and sulfonation

process have a significant effect on the morphology of the composites. The bright field TEM image in Figure 40 shows the optically transparent graphene nanosheets. The carbon element mapping shows the typical image of the graphene sheets. The uniform distribution of sulfur (c) along with carbon over the whole area of the graphene sheet suggested the presence of a homogeneous sulfonated graphene sheets.

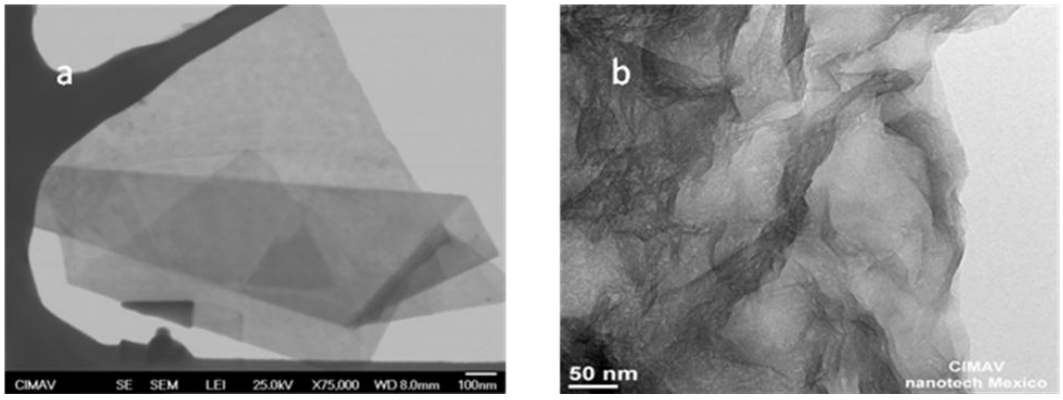

Figure 39. a) Graphene sheets reduced by $KBrH_4$ b) GNSA

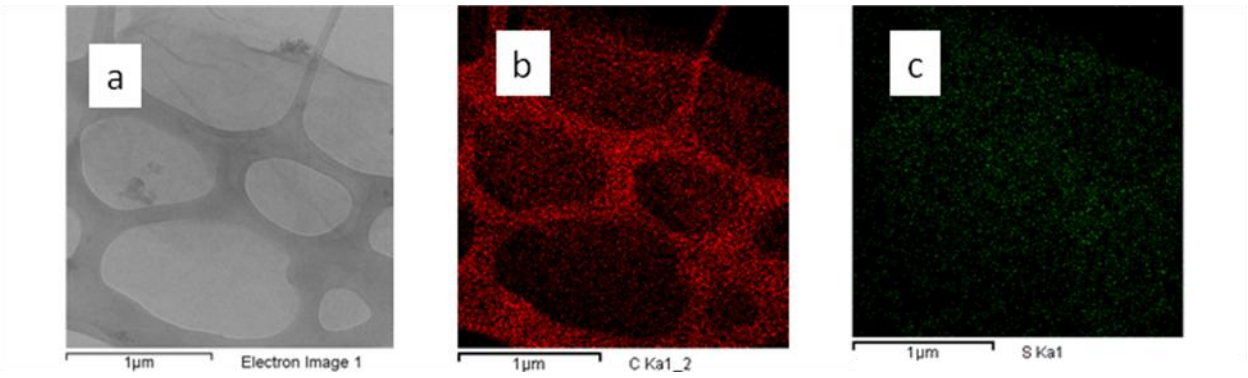

Figure 40. TEM images of the GNSA composites. (a) Zero-energy loss bright field image, (b) carbon element mapping, (c) sulfur element mapping

To determine the distribution and calculate the amount of the C, O, S elements in the material, elemental analyses were run by EDS on the selected areas of the same composite, as seen in Figure 41

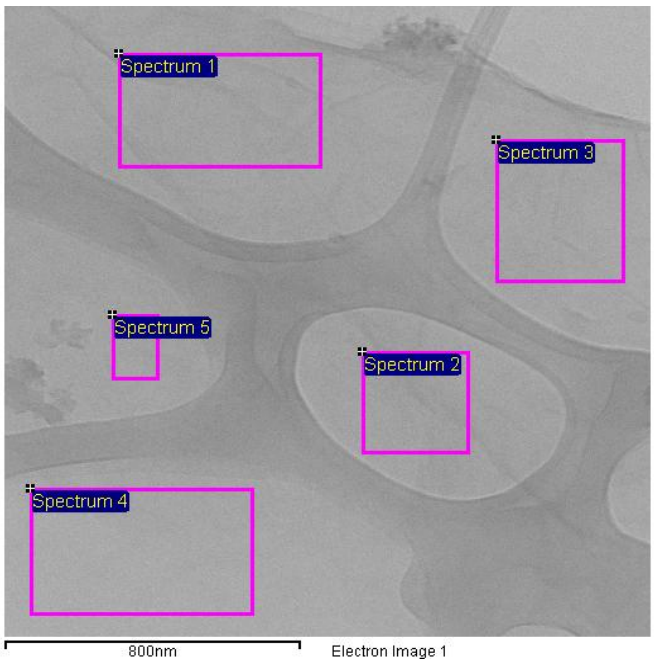

Figure 41. TEM image of the GNSA composite

Table 5. Elemental analysis of the selected areas in Figure 41

Selected Area	C	O	S
Spectrum 1	80. 17	12. 56	4. 07
Spectrum 2	79. 19	12. 23	5. 78
Spectrum 3	84. 44	9. 22	4. 33
Spectrum 4	83. 74	10. 58	3. 53
Spectrum 5	80. 45	12. 32	4. 72
Min Value	80. 17	12. 56	4. 07
Max Value	79. 19	12. 23	5. 78

The results showed that GNSA samples include mostly C, O, and S, respectively. The presence of O suggests the remaining of some oxidized parts on the graphene sheets,

and also presence of NSA in the sample. The ratio of S is a good indicator of the sulfonation efficiency (Coskun *et al.* , 2012).

The bright field TEM image in Figure 42 shows the optically transparent graphene nanosheets and electron diffraction pattern of the sample. As seen in the Figure, on the large area of GNS diffraction the electron diffraction pattern showed changes according to the selected area. In the first and second zones, typical sharp, polycrystalline ring patterns are obtained, which come from (1100) and (1120) plane, respectively (McAlliston *et al.* , 2007). The bright spots correspond to typical hexagonal symmetry of the graphene. In the third zone, a polycrystalline ring can be observed. On the first ring pattern, the number of the diffraction spots increased with respect to the other zones. These results implied that in these parts of the sample, the sheets are more randomly oriented.

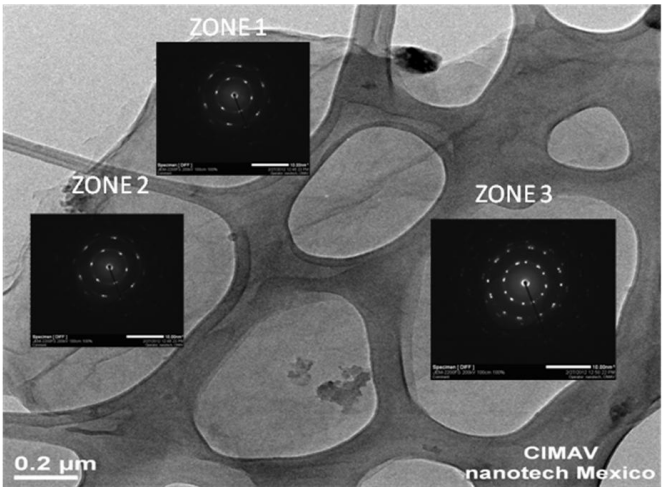

Figure 42. Electron diffraction pattern of the selected areas of the GNSA composite.

The TEM images of the PAni / GNSA composites are shown in Figure 43. Obviously, the morphology of the PAni / GNSA composites was very different than the pure SGrf

ones. As observed, the composites presented high graphene density and uniform morphology, showing some small nanoparticles on the surface of it.

The formation of the composites with PAni by in situ polymerization of aniline in the presence of sulfonated graphene allowed us to prepare homogeneous composites. The composition of PANI and SGrf are believed to intercalate with each other instead of individually being in an agglomerated form as observed previously (Zhang *et al.* , 2010). In Figure 44, polymer particles clearly appear on or between the surfaces of the graphene sheets, while the graphene sheets agglomerates. The dimension of the PAni particles are around 30 nm as reported before (Coskun *et al.* , 2012)

The composite morphology exhibited good interaction of the PAni with the SGrfs. A high-magnification TEM image indicated that the polymer particles are closely attached on the surface of graphene sheets, which can further validate the good interaction between PAni and sulfonated graphene.

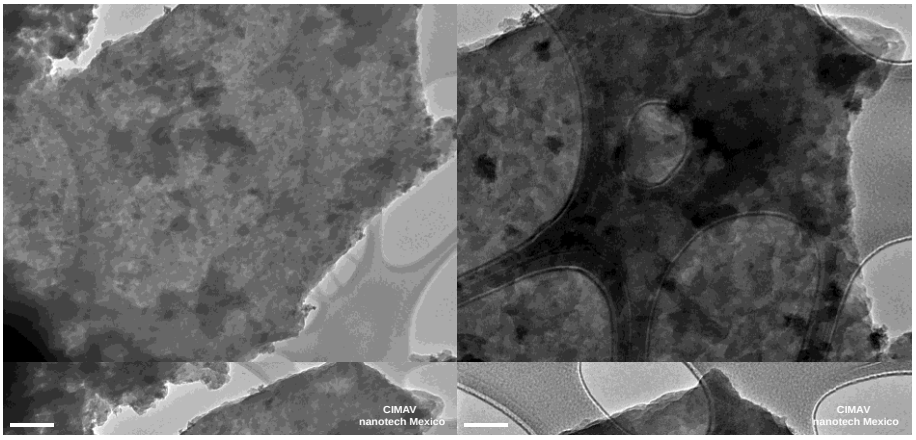

Figure 43. TEM images of the PAni/GNSA composites

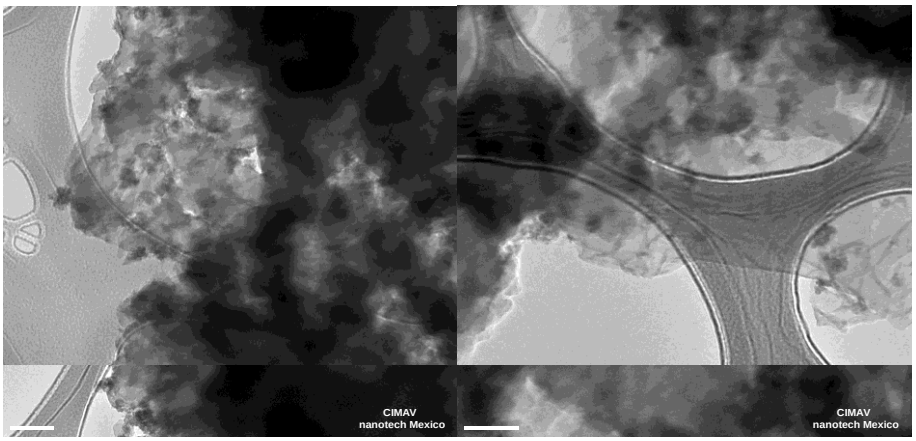

Figure 44. TEM images of PAni/GSA composite

X. CONCLUSIONS

Two convenient methods for dopping PAni with graphene oxide, and another for functionalization of graphene with PAni were developed. According to these methods, PAni / RGO composites and PAni / SGrf composites have been successively prepared, as seen in the characterization results. These strategies are new routes to graphene based materials.

As aimed, in the PAni / RGO composites, reduction of the graphene by leucoemeraldine state of polyaniline, and doping of PAni with reduced graphene was performed at the same time. The final products were obtained as electroactive materials as seen in the voltammograms. The PAni / GO 100 material was the most prominent, which showed closer electrochemical activity to pure PAni.

The sulfonation of graphene by coupling the diazonium salts allowed us to prepare two types of PAni / SGRf composites. These graphene sheets acted as external dopant for PAni. These materials showed better conductivity comparing to pure PAni, and PAni / RGO materials. Coupling with the diazonium salt of NSA gives the highest conductivity in its SGrfs and PAni composites. Furthermore, the sulfonated graphenes showed better electroactivity at higher pH electrolytes than PAni. It points that the, sulfonation method worked for good interconnection between graphene and PAni.

It is believed that these facile syntheses may represent the way for successfully employing PAni-graphene material for electronics applications.

REFERENCES

Affounea A. M. , Prasada B. L. V. , Satoa H. , Enoki T. , Kaburagib Y. , Hishiyama Y. 2001. Experimental evidence of a single nano-graphene. *Chem. Phys. Letters.* 348:17–20.

Bai H. , Xu Y. , Zhao L. , Li C. , Shi G. 2009. Non-covalent functionalization of graphene sheets by sulfonated polyaniline. *Chem. Commun.* 13:1667–1669

Barbero C. , Salavagione H. J. , Acevedo D. F. , Grumelli D. E. , Garay F. , Gabriel A. *et al.* 2004. Novel synthetic methods to produce functionalized conducting polymers I. Polyanilines. *Electrochim. Acta* 49: 3671–3686.

Becerril H. A. , Man J. , Liu Z. , Stoltenberg R. M. , Bao Z. and Chen Y. 2008. Evaluation of solution-processed reduced graphene oxide films as transparent conductors. *ACS Nano* 2: 463-470

Bhadra S. , Khastgira D. , Singha N. K. and Lee J. H. 2009. Progress in preparation, processing and applications of polyaniline. *Prog. Polym. Sci.* 34:783–810.

Bourdo S. and Viswanathan T. 2005. Graphite / Polyaniline (GP) composites: Synthesis and characterization. *Carbon* 43: 2983–2988.

Boyer, M. I. , Quillard, S. , Louarn, G. , Froyer, G. and Lefrant, S. 2000 Vibrational Study of the $FeCl_3$-Doped Dimer of Polyaniline; A Good Model Compound of Emeraldine Salt *J. Phys. Chem.* 104:8952-8961.

Bredas, J. L. , Themans, B. , Andre, J. M. , Chance, R. R. and Silbey, R. 1984. The role of mobile organic radicals and ions (solitons, polarons and bipolarons) in the transport properties of doped conjugated polymers. *Synthetic Met*. 9:265-274.

Chen, G. , Zhai, S. , Zhai, Y. , Zhang, K. , Yue, Q. , Wang, L. , *et al.* 2011. Preparation of sulfonic-functionalized graphene oxide as ion-exchange material and its application into electrochemiluminescence analysis. *Biosens. Bioelectron*. 26(7): 3136-314.

Chiang, J. C. and MacDiarmid, A. G. 1986. Polyaniline': Protonic Acid Doping of the Emeraldine Form to the Metallic Regime. *Synthetic. Met*. 13:193-205.

Choa, H. S. and Park, Y. H. 2004. Preparation and characterization of conducting poly(vinyl chloride)-g-poly(aniline) copolymer. *Synthetic. Met.* 145: 141–146.

Coşkun, E. , Ramírez, S. M. H. , Flores, W. A. , Escobar, C. A. H. , Contreras. , E. A. Z. 2012. Improving polyaniline processability by grafting acrylic copolymer. *Synthetic Met*. 162:344-351

Coşkun, E. , Zaragoza-Contreras, E. A. and Salavagione, H. J. 2012. Synthesis of sulfonated graphene / polyaniline composites with improved electroactivity. *Carbon*. DOI 10. 1016/J. carbon. 2012. 01. 041

Dhand, C. , Das, M. , Datta, M. and Malhotra, B. D. 2011. Recent advances in polyaniline based biosensors. *Biosens Bioelectron.* 26:2811–21.

Diaz, A. F. and Logan, J. A. 1980. Electroactive polyaniline films. *J. Electroanal. Chem.* 111: 111-114.

Dreyer , D. R. , Park , S. C. , Bielawski, W. R. and S. Ruoff . 2010. The chemistry of graphene oxide. *Chem. Soc. Rev.* 39:228.

Du, X. S. , Xiao, M. and Meng Y. Z. 2004. Facile synthesis of highly conductive polyaniline/graphite nanocomposites. *Eur. Polym. J.* 40 :1489–1493.

Eda, G. and Chhowalla, M. 2010. Chemically Derived Graphene Oxide: Towards Large-Area Thin-Film Electronics and Optoelectronics, *Adv. Mater*. 22: 2392-2415.

Eda, G. , Fanchini, G. and Chhowalla M. 2008. Large-area ultrathin films of reduced graphene oxide as a transparent and flexible electronic material. *Nat. Nanotechnol*. 3:270.

Falcao, E. H. L. and Wudl, F. 2007. Carbon allotropes: beyond graphite and diamond. *J Chem. Technol. Biot*. 82:524-531

Feng, X. M. , Li, R. M. , Ma, Y. W. , Chen, R. F. , Shi, N. E. , Fan, Q. L. *et al.* 2011. One-Step Electrochemical Synthesis of Graphene/Polyaniline Composite Film and Its Applications. *Adv. Func. Mater*. 21: 2989-2996.

Ferrari, A. C. , Meyer, J. C. , Scardaci, V. , Casiraghi, C. , Lazzeri, M. , Mauri, F. *et al.* 2006. Raman Spectrum of Graphene and Graphene Layers. *Phys. Rev. Lett.* 97:187401-187405.

Fritsche, J. 1840. Aniline, decomposition product of indigo. *J Prakt Chem* 20: 453

Fu, Y. and Weiss, R. A. 1997. Protonation of polyaniline with lightly sulfonated polystyrene. *Synthetic Met.* 84: 103-104.

Fuhrer, M. S. , Lau, C. N. and MacDonald, A. H. 2010. Graphene: Materially Better *Carbon*. MRS Bulletin. 35 :289-295 doi:10. 1557/mrs2010. 551

Gao, H. , Jiang, T. , Han, B. , Wang, Y. , Du, J. , Liu, Z. and Zhang, J. 2004. Aqueous/ionic liquid interfacial polymerization for preparing polyaniline nanoparticles. *Polymer*. 45:3017-3019

Gerard, M. , Chaubey, A. and Malhotra, B. D. 2002. Application of conducting polymers to biosensors. *Biosens. Bioelectron.* 17: 345-359.

Ghanbari, K. , Mousavi, M. F. , Shamsipur, M and Karami, H. 2007. Synthesis of polyaniline/graphite composite as a cathode of Zn-polyaniline rechargeable battery. *J. Power Sources.* 170 (2):513-519.

Ginder, J. M. and Epstein, A. J. 1990. Role of ring torsion angle in polyaniline: Electronic structure and defect states. *Phys. Rev.* 41:10674-10685.

Gospodinova, N. V. and Terlemezyan, L. 1998. Conducting polymers pre- pared by oxidative polymerization: polyaniline. *Prog. Polym. Sci*. 23:1443-84.

H. Lethebey. 1862. *J. Chem. Soc.* 15:161.

Hao, Q. , Wang, H. , Yang, X. , Lu, L. and Wang, X. 2011. Morphology-Controlled Fabrication of Sulfonated Graphene/Polyaniline Nanocomposites by Liquid/Liquid Interfacial Polymerization and Investigation of their Electrochemical Properties. *Nano Res.* 4: 323–333.

Heeger, A. J. 2001. Semiconducting and Metallic Polymers: The Fourth Generation of Polymeric Materials (Nobel Lecture) *Angew. Chem. Int. Ed.* 40: 2591-2611, 1433-7851.

Hummers, W. S. and Offeman, R. E. 1958. Preparation of Graphitic Oxide. *J. Am. Chem. Soc.* 80:1339-1339.

Kim, J. , Kwon, S. and Ihm, D. W. 2007. Synthesis and characterization of organic soluble polyaniline prepared by one-step emulsion polymerization. *Curr. Appl. Phys.* 7: 205–210.

Kinlen P. J. , Frushour, B. G. , Ding, Y. and Menon, V. 1999. Synthesis and characterization of organically soluble polyaniline and polyaniline block copolymers. *Synth. Met*. 10:758–761.

Kinlen, P. J. , Liu, J. , Ding, Y. , Graham, C. R. and Remsen, E. E. 1998. Emulsion polymerization process for organically soluble and electrically conducting polyaniline. *Macromolecules*. 31:1735–1744.

Kumar, D. , Pathak, M. , Srivastava, M. , Naveen, K, Himanshu, K. and Shivam, A. 2011. Conductive polymers. *J. Text. Assoc.* 72:159-166

Lee, S. , Lee, K. and Zhong, Z. 2010. Wafer Scale homogeneous bilayer graphene films by chemical vapor deposition. *Nano Lett.* 10:4702.

Li, D. , Muller, M. B. , Gilje, S. , Kaner, R. B. and Wallace, G. G. 2008. Processable aqueous dispersion of graphene nanosheets. *Nat. Nanotechnol*. 3:101–5.

Li, W. , Johnson, C. L. and Wang, H. L. 2004. Preparation and characterization of monolithic polyaniline–graphite composite actuators. *Polymer.* 45:4769–4775.

Lomeda, J. R. , Doyle, C. D. , Kosynkin, D. V. , Hwang, W. F. and Tour, J. M. 2008. Diazonium functionalization of surfactant-wrapped chemically converted graphene sheets *J. Am. Chem. Soc.* 130: 16201-16206.

Lotya, M. , Hernandez, Y. , King, P. J. , Smith, R. J. , Nicolosi, V. and Karlsson, V. L. S. 2009. Liquid Phase Production of Graphene by Exfoliation of Graphite in Surfactant/Water Solutions. *J. Am. Chem. Soc.* 131: 3611-3620.

Macdiarmid, A. G. ,Yang, L. S. , Huang, W. S. and Humphery, P. D. 1987. Polyaniline: Electrochemistry and application to rechargeable batteries *Synthetic Met.* 18: 393-398

MacDiarmid and A. G. 2001. Synthetic Metals: A Novel Role for Organic Polymers (Nobel Lecture). *Angew. Chem. Int. Ed.* 40: 2581- 2590.

MacDiarmid, A. G. , Jones, J. W. E. , Norris, I. D. , Gao, J. , Johnson, J. A. T. , Pinto, N. J. , *et al.* 2001. Electrostatically-Generated Nanofibers of Electronic Polymers. *Synthetic Met.* 119: 27-30.

Malesevic, A. , Vitchev, R. , Schouteden, K. , Volodin, A. , Zhang, L. and Tendeloo, G. V. 2008. Synthesis of few-layer graphene via microwave plasma-enhanced chemical vapour deposition. *Nanotechnolgy.* 19:305604.

Masters, J. G. , Sun, Y. , MacDiarmid, A. G. and Epstein, A. J. 1991. Polyaniline: Allowed oxidation states. *Synthetic Met*. 41: 715-718.

McAllister, M. J. , Li, J. L. , Adamson, D. H. , Schniepp, H. C. , Abdala, A. A. , Liu, J. , Alonso, M. H *et al.* 2007. Single Sheet Functionalized Graphene by Oxidation and Thermal Expansion of Graphite. *Chem. Mater.* 19: 4396–4404

Mohilner, D. , M. , Adams, R. N. and Argensinger, W. J. 1962. Investigation of kinetics and mechanism of anodic oxidation os aniline in aqueous sulfuric acid solution at a platinum electrode. *J. Am. Chem. Soc*. 84: 3618-3622.

Niyogi, S. , Bekyarova, E. , Itikis, M. E. , McWilliams, J. L. , Hammon, M. A. and Haddon, R. C. 2006. Solution Properties of Graphite and Graphene *J. Am. Chem. Soc.* 128: 7720–7721.

Novoselov, K. S. , Geim, A. K. , Morozov, S. V. , Jiang, D. , Zhang, Y. , Dubonos, S. V. *et al.* 2004. Electric Field Effect in Atomically Thin Carbon. *Science.* 306: 666-669.

Österholm, J. E. , Cao, Y. , Klavetter, F. and Smith, P. 1993. Emulsion polymerization of aniline. *Synthetic Met*. 55: 1034–1039.

Österholm, J. E. , Cao, Y. , Klavetter, F. and Smith, P. 1994. Emulsion polymerization of aniline. *Polymer* 35: 2902–2906.

Potts, J. R. , Dreyer, D. R. , Bielawski, C. W. , Rodney S. and Ruoff, R. S. 2011. Graphene-based polymer nanocomposites. *Polymer*. 52:5-25.

Quillard, S. , Louarn, G. and Lefrant, S. 1994. Vibrational analysis of polyaniline: A comparative study of leucoemeraldine, emeraldine, and pernigraniline bases, *Phys. Rev*. B 50 :12496. 12508.

Ramanathan, A. A. , Abdala, S. , Stankovich, D. A. , Dikin, M. , Herrera-Alonso, R. D. , Piner, D. H. *et al.* 2008. Functionalized graphene sheets for polymer nanocomposites, *Nat. Nanotechnol.* 3*: 327 – 331.*

Salavagione, H. J. , Morales, G. M. , Miras, M. C. and Barbero, C. 1999. Novel synthetic methods to produce functionalized conducting polymers I. Polyanilines *Acta Polym.* 50:40-44.

Salavagione, H. J. , Acevedo, D. F. , Miras, M. C. and Barbero, C. 2003. Redox coupled Ion Exchange in copolymers of Anyline with Aminobenzoic Acids. *Port. Electrochim. Acta,* 21: 245-254.

Sanchís, C. , Salavagione, H. J. , and Morallón, E. 2008. Ferrocenium strong adsorption on sulfonated polyaniline modified electrodes. *J. Electroanal. Chem.* 618: 67-73.

Savitha, P. and Sathyanarayana, D. N. 2004. Synthesis and characterization of soluble conducting poly(*o*-/*m*-toluidine-*co*-*o*-nitroaniline). *Synthetic Met*. 145: 113–118.

Schniepp, H. C. , Li, J. L. , McAllister, M. J. , Sai, H. , Herrera-Alonso, M. , Adamson, D. H. , *et al.* 2006. Functionalized Single Graphene Sheets Derived from Splitting Graphite Oxide, *J. Phys. Chem. B* 110:8535–8539.

Shirakawa, H. 2001. The discovery of polyacetylene film: the dawning of an era of conducting polymers (Nobel Lecture). *Angew. Chem. Int. Ed.* 40: 2575-2580, 1433-7851.

Shirakawa, H. , Louis, E. J. , MacDiarmid, A. G. , Chiang, C. K. and Heeger, A. J. 1977. Synthesis of electrically conducting organic polymers: Halogen derivatives of polyacetylene. *J. Chem. Soc. Chem. Commun.* 16: 578-580.

Si, Y. and Samulski, E. T. 2008. Synthesis of Water Soluble Graphene. *Nanoletters.*

8: 1679-1682

Singh, V. , Joung, D. , Zhai, L. , Das, S. , Khondaker, S. I. and Seal, S. 2011. Graphene based materials: Past, present and future. *Prog. Mater. Sci.* 56 :1178–1271.

Smits, F. M. 1958 . *The Bell System Technical Journal* 37: 711-718.

Stafstrom, S. , Bredas, J. L. , Epstein, A. J. , Woo, H. S. , Tanner, D. B. , Huang, W. S. *et al.* 1987. Polaron lattice in highly conducting polyaniline: Theoretical and optical studies. *Phys. Rev. Lett*. 59:1464-1467.

Stankovich, S. , Dikin, D. A. , Piner, R. D. , Kohlhaas, K. A. , Kleinhammes, A, and Jia, Y. 2007. Synthesis of graphene-based nanosheets via chemical reduction of exfoliated graphite oxide. *Carbon.* 45:1558.

Stankovich, S. , Piner, R. D. , Chen, X. , Wu, N. , Nguyen, S. T. and Ruoff, R. S. 2006 Stable aqueous dispersions of graphitic nanoplatelets *via* the reduction of exfoliated graphite oxide in the presence of poly(sodium 4-styrenesulfonate). *J. Mater. Chem.* 16: 155–158.

Stejskal ,J. and Sapurina, I. 2008. Polyaniline-a conducting polymer. *Materials syntheses. Wien: Springer*: 199-207.

Stejskal, J. 2002. Polyaniline, Preparation of a conducting Polymer, IUPAC technical Report. *Pure Appl. Chem*. 74 :857-867.

Trchová, M. and Stejskal, J. 2011. The infrared spectroscopy *of conducting polymer nanotubes. Pure Appl. Chem.* 83: 1803-1807.

Tung, V. C. , Allen, M. J. ,Yang,Y. and Kaner, R. B. 2009. High-throughput solution processing of large-scale graphene, *Nat. Nanotechnol*. 4:25-29.

Vallés, C. , Jimenez, P. , Muñoz, E. , Benito, A. M. and Maser, W. K. 2011. Simultaneous Reduction of Graphene Oxide and Polyaniline: Doping-Assisted Formation of a Solid-State Charge-Transfer Complex , *J. Phys. Chem.* 115:10468–10474.

Vitchev, R. , Malesevic, A. , Petrov, R. H. , Kemps, R. , Mertens, M. and Vanhulsel, A. 2010. Initial stages of few-layer graphene growthby microwave plasma-enhanced chemical vapour deposition. *Nanotechnol.* 21:095602.

Wallace, G. G. , Lewis, T. W. , and Kane-Maguire, L. A. P. 2002 “Conductive Polymers,” *Encyclopedia of Smart Materials*, John Wiley and Sons, 279-291.

Wang, D. W. , Li, F. , Zhao, J. , Ren, W. , Chen, Z. G. , Tan, J. *et al.* 2009. Fabrication of Graphene/Polyaniline Composite Paper *via In Situ* Anodic Electropolymerization for High-Performance Flexible Electrode. *ACS Nano*. 3: 1745-1752.

Wang, H. , Hao. , Q. , Yang, X. , Lu, L. and Wang, X. 2009. Graphene oxide doped polyaniline for supercapacitors. *Electrochem. Commun.* 11: 1158–1161.

Wang, H. , Hao. , Q. , Yang, X. , Lu, L. and Wang, X. 2010 A nanostructured graphene/polyaniline hybrid material for supercapacitors. *Nanoscale.* 2: 2164-2170.

Wang, X. , Jin, X. , Dawei, G. , Shen, L. 2006A novel Zn-PANI dry rechargeable battery. *Rare Metals.* 25 (6): 67-70.

Wanga, Y. , Shia, Y. , Xua, X. , Liua, F. , Yaoa, H. , Zhaia, G. *et al.* 2009. Preparation of PAni-coated poly (styrene-co-styrene sulfonate) nanoparticles inmicroemulsion media, Colloids and Surfaces A*: Physicochem. Eng. Aspects*. 345:71–74.

Wise, D. L. , Wnek, G. E. , Trantolo, D. L. , Cooper T. M. and Gresser, J. D. 1998. Electrical and optical polymer System. Fundamentals, Methods and Applications. New York. p: 775.

Yan, X. , Chen, J. , Jie Yang, J. , Xue, Q. and Miele, P. 2010. Fabrication of Free-Standing, Electrochemically Active, and BiocompatibleGraphene Oxide-Polyaniline and Graphene-Polyaniline Hybrid Papers. *ACS Appl. Mat*. 2: 2521–2529.

Yang, N. , Zhai, J. , Wan, M. , Wang, D. , Jiang, L. 2010. *Synthetic Met.* 160: 1617-1622.

Zhang, K. , Zhang, L. L. , Zhao, X. S. and Jishan, W. 2010. Graphene/Polyaniline Nanofiber Composites as Supercapacitor Electrodes. *Chem. Mater.* 22:1392–1401.

Zhao, G. , Jiang, L. , He, Y. , Li J. , Dong, H. and Wang, X. 2011. Sulfonated graphene for persistent aromatic pollutant management. *Adv Mater*. 23:3959–63.

Zhu, Y. , Higginbotham, A. L. and Tour, J. M. 2009. Covalent Functionalization of Surfactant-Wrapped Graphene Nanoribbons. *Chem. Mater.* 21: 5284-5291.

Zhu, Y. , Murali, S. ,Cai, W. , Li, X. , Suk, J. W. , R. Potts, J. R. , and Ruoff, *S. R*. 2010. Graphene and Graphene Oxide: Synthesis, Properties, and Applications. *Adv. Mater. 22*:3906–3924.